

In presenting the dissertation as a partial fulfillment of the requirements for an advanced degree from the Georgia Institute of Technology, I agree that the Library of the Institute shall make it available for inspection and circulation in accordance with its regulations governing materials of this type. I agree that permission to copy from, or to publish from, this dissertation may be granted by the professor under whose direction it was written, or, in his absence, by the Dean of the Graduate Division when such copying or publication is solely for scholarly purposes and does not involve potential financial gain. It is understood that any copying from, or publication of, this dissertation which involves potential financial gain will not be allowed without written permission.

7

7/25/68

DETERMINATION OF THE ELECTRIC DIPOLE
MOMENTS OF CFCl_3 AND CHCl_3

A THESIS

Presented to

The Faculty of the Graduate Division

by

Philip Benton Reinhart

In Partial Fulfillment

of the Requirements for the Degree

Doctor of Philosophy in the School of Physics

Georgia Institute of Technology

August, 1968

DETERMINATION OF THE ELECTRIC
 DIPOLE MOMENT OF
 CFCl_3 AND CHCl_3

Approved:

Chairman, _____

Date approved by Chairman: 12/31/68

ACKNOWLEDGEMENTS

The author is grateful to Drs. J. Q. Williams and T. L. Weatherly for their patient supervision and for the privilege of working in the microwave group.

The author is also grateful to Agnes Scott College for its support -- financial and otherwise -- of this Ph.D. program. This research was supported in part by a Science Faculty Fellowship from the National Science Foundation and in part by a National Aeronautics and Space Administration Institutional Grant.

TABLE OF CONTENTS

	Page
ACKNOWLEDGEMENTS	ii
LIST OF TABLES	v
LIST OF ILLUSTRATIONS	vi
Chapter	
I. INTRODUCTION	1
II. DATA COLLECTION PROCEDURES	4
Tuning Techniques and Frequency Measurements (Method 1)	
Tuning Techniques and Frequency Measurements (Method 2)	
Processing the Detector Output	
Data Gathering Techniques	
III. THEORY	24
Quadrupole Interaction Theory	
The Combined Stark and Quadrupole Interaction	
Stark Effect in the Absence of Quadrupole Splitting	
Pressure Broadening	
IV. ANALYSIS OF DATA	46
Electric Dipole Moment Determinations	
Comparison of Observed with Calculated Spectra	
V. CONCLUSIONS AND RECOMMENDATIONS	64
APPENDIX A	66
APPENDIX B	69
APPENDIX C	72
APPENDIX D	76

TABLE OF CONTENTS (Continued)

Chapter	Page
APPENDIX E	91
LITERATURE CITED	103
VITA.	105

LIST OF TABLES

Table		Page
1.	Electric Dipole Moments of CHCl_3 and CFCl_3 in the Gaseous State	54
2.	Frequencies of the High Intensity Lines in the $J = 2 - 3$ Transitions	63
3.	The Permutation Group on Three Objects	73
4.	The Genealogical Coefficients	74
5.	The Reduction Coefficients	75

LIST OF ILLUSTRATIONS

Figure		Page
1.	Synchronizer Circuits	7
2.	Vector Diagrams for the Phase Comparator	9
3.	The Creation of a 30 MHz Beat Note by Mixing Three Signals: A, B, C	11
4.	Equipment Set-up for the Beat Note Technique	15
5.	Beat Note Markers on a Recording Chart	17
6.	Processing of the 30 KHz Signal from the Crystal Detector	19
7.	30 KHz Signals Involved in Processing Detector Output	20
8.	Vector Diagrams Illustrating Phase Comparator Voltages Under Stark Modulation	21
9.	Form of Hamiltonian Matrix in the Representation of Equation III-5.	32
10.	The Form of a Typical Submatrix when Spin Functions, $u(w_k I)$, are used	34
11.	Form of Hamiltonian Matrix for Combined Stark and Quadrupole Interaction.	41
12.	Form of Hamiltonian Matrix for Combined Stark and Quadrupole Interaction when Basis Functions are Symmetrized.	42
13.	Stark Components of CHCl_3 Measured by Double Phase Lock Stabilization Method	49
14.	Stark Components of CFCl_3 Measured by Double Phase Lock Stabilization Method	50
15.	Second Stark Components of CHCl_3 Measured by Beat Note Method.	52
16.	Second Stark Components of CFCl_3 Measured by Beat Note Method.	53

LIST OF ILLUSTRATIONS (Continued)

Figure		Page
17.	Calculated Pressure Broadened Spectrum for the $J = 2 - 3$ Transition of CHCl_3	56
18.	Calculated Pressure Broadened Spectrum for the $J = 2 - 3$ Transition of CHCl_3	57
19.	Calculated Pressure Broadened Spectrum for the $J = 2 - 3$ Transition of CHCl_3	58
20.	Calculated Pressure Broadened Spectrum for the $J = 2 - 3$ Transition of CHCl_3	59
21.	Measured Spectrum of CHCl_3	60
22.	Calculated Pressure Broadened Spectrum for the $J = 2 - 3$ Transition of CFCI_3	61
23.	Measured Spectrum of CFCI_3	62
24.	Program Segment	96
25.	Computer Variables and Associated Physical Quantities	99
26.	The $J = 2$, $M_F = 9/2$, $K = 1$ Submatrix	101
27.	Form of Eigenvector Corresponding to the K_1 -th Eigenvalue of the $J = 2$, $K = 1$, $M_F = 9/2$ Submatrix	102

CHAPTER I

INTRODUCTION

In recent years one of the interests of the microwave group at Georgia Institute of Technology has been the study of the microwave spectra of symmetric top molecules having three identical quadrupolar nuclei. A. A. Wolf (1) studied the quadrupole hyperfine structure in the $J = 1$ to 2 and the $J = 2$ to 3 rotational transitions of CHCl_3 and CFCl_3 . From his work he obtained values for the quadrupole coupling constants, eqQ , and the rotational constants, B , for both molecules. C. R. Nave (2) studied the spectrum resulting from the combined Stark and quadrupole interactions in the $J = 1$ to 2 rotational transitions in PCl_3 and POCl_3 and obtained values for the dipole moments of both these molecules.

The quadrupole interaction theory used by the above researchers was originally developed by Svidzinski (3). Wolf made some corrections to Svidzinski's work and applied the corrected theory to his own data. Nave extended the theory as used by Wolf to include the Stark interaction for the $J = 1$ to 2 transition and applied this theory to PCl_3 and POCl_3 .

The original objective of the research reported here was to determine values for the quadrupole coupling constant and the dipole moment of the symmetric top molecule, bromoform (CHBr_3). The $J = 2$ to 3 rotational transition of CHBr_3 is the lowest that can be studied with present equipment in the microwave group. Therefore, the Stark plus quadrupole interaction theory used by Nave was

extended to cover this transition.

Unfortunately, efforts to measure the $J = 2$ to 3 transition in CHBr_3 were unsuccessful. The intensity of the spectrum was too weak to be observed with present equipment. For this reason, the attempt to study CHBr_3 was abandoned, and a new objective determined. The new objective was threefold: to develop the theory used by Nave to apply to the $J = 2$ to 3 transition in CHCl_3 and CFCl_3 , to check its validity for this transition, and to determine the dipole moments of these molecules.

As far as this researcher can ascertain, no microwave measurements of the dipole moments of these molecules have been made to date. A. L. McClellan (4) lists values that several researchers have found for the dipole moments of CHCl_3 and CFCl_3 . These values range from 0.9 debye to 1.86 debye for CHCl_3 and were obtained from measurements of the dielectric constant of that molecule in its gaseous state. Two values for the dipole moment of CFCl_3 have been reported, 0.45 debye and 0.53 debye using the same method. Microwave determinations of dipole moments are much more accurate than dielectric determinations (5).

Checking the validity of the $J = 2$ to 3 theory for the combined Stark and quadrupole interactions requires accurate knowledge of the bond angle, the quadrupole coupling constant, the Stark field, and the dipole moment of the molecule in question. The bond angles used in the calculation are those found by Loubser (6) and by Jen and Lide (7). The quadrupole coupling constants are those found by A. A. Wolf. Although P. N. Wolf (8) and Long (9) made microwave determinations of eqQ , these values were not used because A. A. Wolf has shown that the

theory used by these researchers in their determinations was incomplete (10). The dipole moments and the Stark fields used in checking the theory are those measured by the author.

Data were taken with a Stark modulated spectrograph. Data gathering techniques and operating principles of the Stark modulated spectrograph are discussed in Chapter II. In Chapter III, relevant theory and its application to dipole moment determinations are discussed. In Chapter IV, computer programs and analysis of data are discussed, and in Chapter V results are summarized.

CHAPTER II

DATA COLLECTION PROCEDURES

The equipment used in this research was a conventional Stark modulated spectrograph, which has been described by Clayton (11), Long (12), and Nave (2). This type of spectrograph is very sensitive and accurate, and it is well suited to the measurement of weak lines. In this chapter, attention is given to electronic design features which result in such sensitivity and accuracy and to the data collection procedures used in this research.

A gas whose microwave spectrum is to be studied is contained at low pressure in the Stark cell of the spectrograph. This cell is a 17 foot length of rectangular waveguide in which a conducting plate or septum has been inserted. The septum extends the entire length of the waveguide and is electrically insulated from the waveguide walls. The plane of the septum is parallel to the broad dimension of the waveguide. The spacing between the septum and either parallel wall is 0.481 cm (13). A 30 kHz square-wave voltage is applied between the septum and the walls of the cell. The effect of the square-wave voltage is to subject the gas alternately to a Stark electric field of 0 volts/cm and $V/0.481$ volts/cm, where V is the amplitude of the square-wave voltage. The gas in the cell is kept at low temperature by placing dry ice on top of the waveguide.

Microwave energy is emitted into the Stark cell at one end. This energy comes from a klystron oscillator which is tuned slowly over the frequency range

of interest. At the other end of the Stark cell is a crystal detector. The microwave power at the detector will fluctuate at the rate of 30 kHz if the amount of incoming microwave energy absorbed by the gas is different for the Stark-field-on case and the Stark-field-off case. The magnitude and phase (with respect to the square-wave voltage on the Stark electrode) of the 30 kHz signal at the detector is electronically determined, and this information is displayed graphically by an Esterline Angus graphic ammeter.

A detailed accounting is given below to the two different techniques used to tune the klystron and to measure its frequency and to the manner in which the 30 kHz signal is processed.

Tuning Techniques and Frequency Measurements (Method #1)

Part of the measurements were made using a double phase-lock stabilization technique to tune the klystron over the frequency ranges of interest. This technique involves the use of two klystrons, a source klystron and reference klystron, and has been described by Narath and Gwinn (14), and by Nave (15). Here the technique is illustrated by an example.

While studying the spectrum of CHCl_3 it was necessary to tune the source klystron from 19.810 GHz to 19.870 GHz. This tuning was achieved by first stabilizing the reference klystron at 9.830 GHz, then phase-locking the source klystron at 19.810 GHz, and finally tuning the source klystron over the frequency range, 19.810 to 19.870 GHz. The techniques involved are discussed below.

Stabilizing the Reference Klystron at 9.830 GHz

With a model DY-2650A Dymec Oscillator Synchronizer, a klystron can

be stabilized at any frequency at which it can oscillate and which satisfies the relation

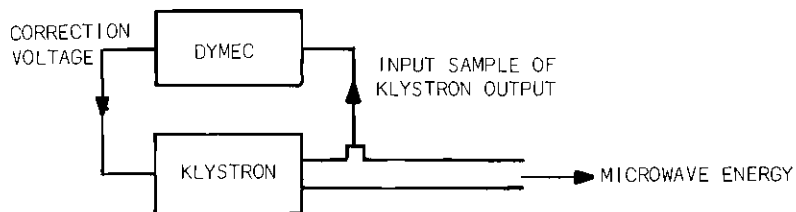
$$\text{FREQUENCY} = N \times 100 \text{ MHz} \pm 30 \text{ MHz} \quad (\text{II-1})$$

where N is any positive integer less 124.

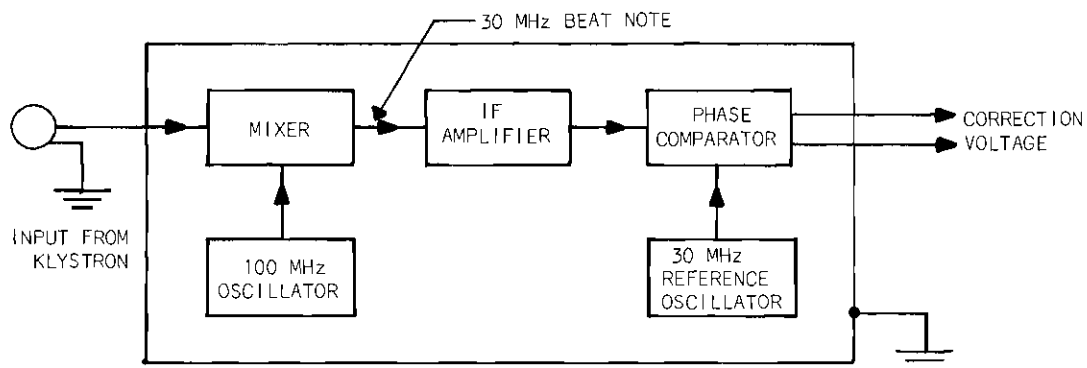
Figure 1a shows how a klystron whose frequency is to be stabilized is connected to the Dymec Synchronizer. A fraction of the microwave energy leaving the klystron is fed to the input terminals of the Dymec. If the klystron is oscillating at a frequency satisfying equation II-1, then no correction voltage is developed. (See discussion about phase below.) If the klystron has begun to drift, then a correction voltage is developed by the Dymec, and this voltage is applied to the reflector of the klystron to correct the drift.

Figure 1b is a block diagram illustrating what happens inside the Dymec. The incoming 9.830 GHz microwave signal is mixed with all the harmonics of an internally generated 100 MHz signal. One of these harmonics (in this case the 98 th harmonic) beats with the microwave frequency to produce a 30 MHz beat note. This beat note is amplified in the IF amplifier section of the synchronizer. The amplified 30 MHz beat note and an independent internally generated 30 MHz reference signal are fed to the phase comparator section.

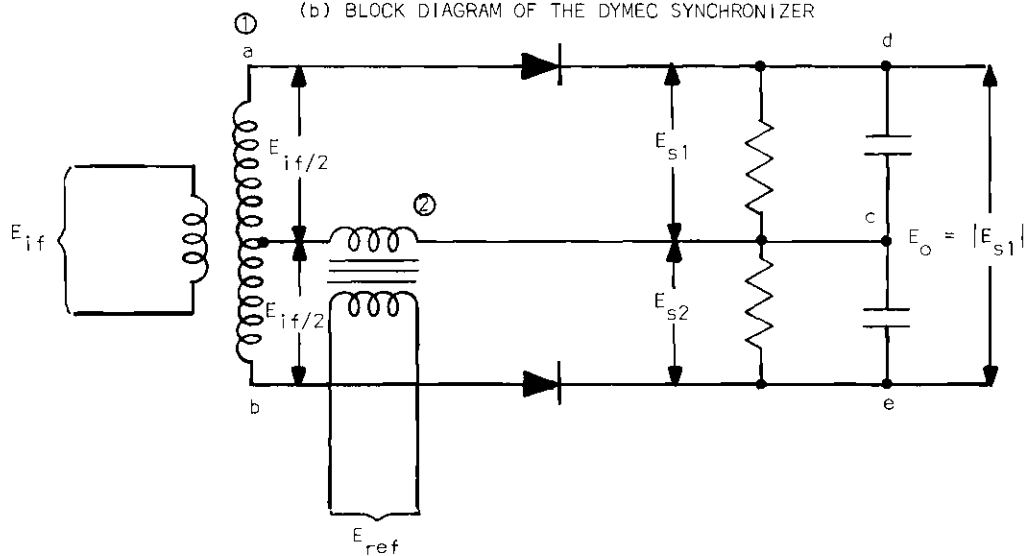
If the two 30 MHz signals are exactly 90° out of phase, then no error voltage is generated by the comparator. If on the other hand, the klystron has begun to drift, thereby causing the phase relationship between the two 30 MHz signals to change from 90° , then a correction voltage is developed by the phase comparator,



(a) CONNECTION OF THE KLYSTRON TO THE SYNCHRONIZER



(b) BLOCK DIAGRAM OF THE DYMEC SYNCHRONIZER



(c) PHASE COMPARATOR CIRCUIT IN THE DYMEC SYNCHRONIZER

Figure 1. Synchronizer Circuits.

and this voltage is applied to the reflector of the klystron to correct the drift.

Phase Comparator. Figure 1c illustrates the phase comparator circuit.

The 30 MHz beat note is fed into the tuned circuit of the phase comparator at 1.

The voltages at a and b are equal in magnitude, $(E_{if}/2)$, and 180° out of phase.

Because of the diode in the upper half of the circuit, the capacitor between c and d can only be charged by the two voltages: E_{ref} and $(E_{if}/2)_a$. Because of the high resistance between c and d, this capacitor cannot significantly discharge during the time interval of the period of the 30 MHz reference signal. The voltage across this capacitor, therefore, reaches a value which is the magnitude of the vector sum of E_{ref} (max) and $(E_{if}/2)_a$ (max),

$$|E_{S1}| = \text{voltage across c-d} = |\vec{E}_{ref} + (\vec{E}_{if/2})_a| . \quad (\text{II-2})$$

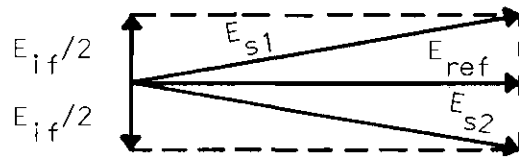
Similarly, the diode, resistor, and capacitor in the bottom half of the circuit result in the voltage across e-c being equal to the magnitude of the vector sum of E_{ref} (max) and $(E_{if}/2)_b$ (max),

$$|E_{S2}| = \text{voltage across e-c} = |\vec{E}_{ref} + (\vec{E}_{if/2})_b| . \quad (\text{II-3})$$

From the vector diagrams in Figure 2 it can be seen that if E_{ref} is 90° out of phase with E_{if} , then $|E_{S1}| = |E_{S2}|$ and the correction voltage is

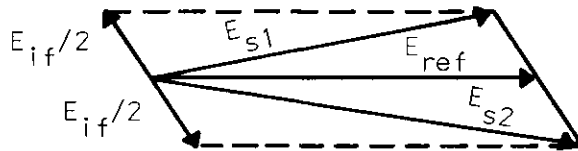
$$E_o = \text{correction voltage} = |E_{S1}| - |E_{S2}| = 0.$$

But, if the phase difference is other than 90° , then a correction voltage is generated. This correction voltage properly applied to the klystron reflector corrects



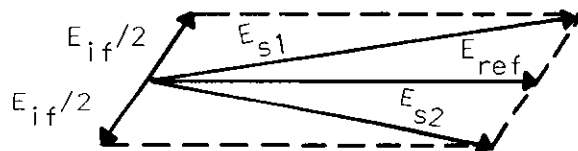
$$E_O = |E_{s1}| - |E_{s2}| = 0$$

(a) ZERO VOLTAGE OUT



$$E_O = |E_{s1}| - |E_{s2}| < 0$$

(b) NEGATIVE VOLTAGE OUT



$$E_O = |E_{s1}| - |E_{s2}| > 0$$

(c) POSITIVE VOLTAGE OUT

Figure 2. Vector Diagrams for the Phase Comparator.

the klystron drift, which was the cause of the phase shift.

Thus, once the reference klystron is locked-in at 9.830 GHz, it is stabilized at that frequency.

Phase-locking the Source Klystron at 19.810 GHz

Phase-lock stabilization of the source klystron at 19.810 GHz involves principles similar to those involved in phase lock stabilization described for the reference klystron. As in the case of the reference klystron, the correction voltage applied to the reflector of the source klystron is developed by the phase comparator section of a Dymec Synchronizer. The phase comparator compares two MHz signals - an internally generated reference signal and a 30 MHz beat note amplified in the IF section.

However, in phase-lock stabilization of the source klystron, the 30 MHz beat note is produced outside of the Dymec and fed directly into the IF section bypassing the Dymec Mixer section. The 30 MHz beat note is the result of mixing three signals in a crystal mixer: a sample of the 19.810 GHz output of the source klystron, the 9.830 GHz output of the reference klystron, and a 120 MHz signal from a variable frequency oscillator (a Hewlett-Packard Transfer Oscillator tunable from 100 to 200 MHz). Figure 3 shows how a 30 MHz beat note results from mixing the three signals.

If the source klystron drifts, then the beat note will drift and the phase comparator will generate a correction voltage which will correct the klystron's drift. Thus, the source klystron is phase-locked at 19.810 GHz.

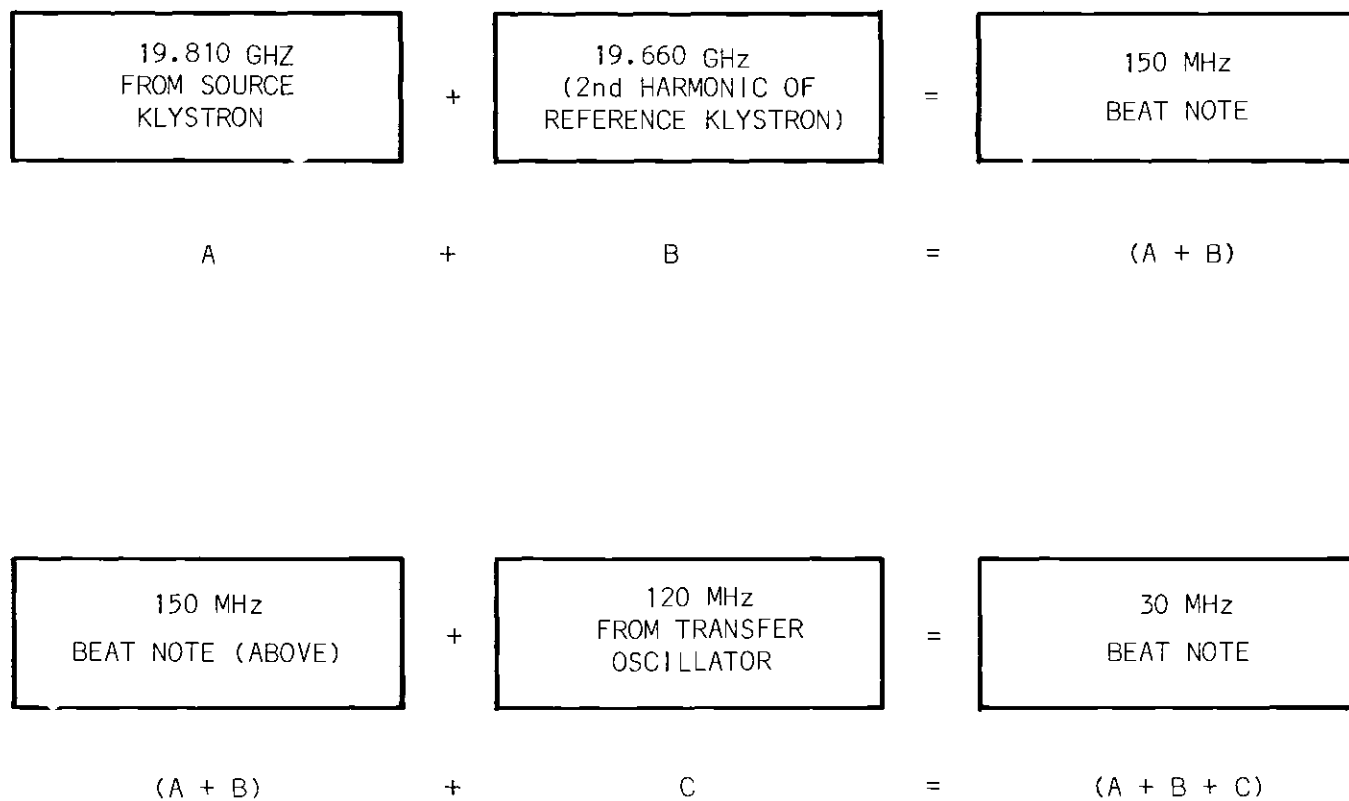


Figure 3. The Creation of a 30 MHz Beat Note by Mixing Three Signals: A, B, C.

Tuning the Source Klystron

If the transfer oscillator frequency is slowly changed, then the 30 MHz beat note will tend to change, and the correction voltage generated by the Dymec will cause the frequency of the source klystron to change in such a way that the 30 MHz beat note maintains its frequency and 90° phase relationship with the Dymec 30 MHz reference signal.

For example, if the transfer oscillator is tuned from 120 MHz to 121 MHz, then in order to maintain the 30 MHz beat note the source klystron frequency must be corrected from 19.810 to 19.811 GHz.

The source klystron was tuned from 19.810 GHz to 19.870 GHz by slowly tuning the transfer oscillator from 120 to 180 MHz. Because the error voltage generated by the phase comparator was not sufficient in magnitude to electrically tune the klystron over the entire range of interest, it was necessary to connect the correction voltage not only to the reflector of the source klystron but also to a switching device that controlled a motor which mechanically tuned the klystron when error voltages were generated.

Frequency Measurements

To determine precisely the source klystron frequency it is necessary to know the exact frequencies of the reference klystron and the transfer oscillator and to know the lock-in scheme (i.e. the relationship among the source klystron, reference klystron, and transfer oscillator frequencies).

The reference klystron frequency is determined approximately by a wave-meter measurement and inferred exactly from the knowledge that this frequency

must satisfy equation II-1. The accuracy of the wave meter is sufficient to enable a determination of N .

The transfer oscillator frequency is measured exactly by a Hewlett-Packard 5245 L Electronic Counter. The counter works as follows: an extremely stable internal crystal oscillator generates a 1 MHz signal. The transfer oscillator signal is mixed with a harmonic of that 1 MHz signal. One can select which harmonic is mixed from any of the following frequencies: 50, 60, 70, ... 500 MHz. The lowest frequency harmonic is chosen such that the beat note formed has frequency between 0 and 13 MHz. The counter counts the number of cycles in the beat note for one tenth of a second (measured against the internally generated 1 MHz signal) and periodically displays the result. From a knowledge of this count and knowledge of the frequency of the harmonic, the transfer oscillator frequency can be inferred.

The lock-in scheme for the source oscillator can be determined from a rough measurement of its frequency with a wave meter and from knowledge of the frequencies of the transfer oscillator and the reference klystron. Once the above is known the exact source frequency can be inferred. An example illustrating the technique is discussed in Appendix A.

Accuracy of Frequency Measurements (Method #1)

The precision to which the source frequency can be determined is related to the precision to which the frequencies of the transfer oscillator and the reference klystron can be determined. One source of error in the determination of the transfer oscillator's frequency results from drift in the 1 MHz crystal in the HP

Electronic Counter. This signal was compared with the signal from WWVB (at 60 kHz) and found to be accurate to one part in 10^8 .

Another possible source of error is drift in the 100 MHz crystal oscillator in the Dymec which controls the reference klystron frequency. This oscillator has been found to be accurate to one part in 10^7 .

Tuning Techniques and Frequency Measurements (Method #2)

An alternative method for tuning the source klystron and for measuring its frequency is to use a beat note technique. In this technique the equipment is set-up as shown in Figure 4.

The klystron is tuned mechanically by a slow motor. Unlike tuning in the double phase-lock stabilization technique, there is no electric tuning or stabilization of the source klystron by application of correction voltages to the reflector.

Frequencies are measured by mixing the outputs of the source klystron and a Micro-Now Frequency Multiplier Chain. The fundamental frequency of the Multiplier Chain can be set to any frequency in the interval 4.979 MHz to 5.006 MHz. During an experiment this frequency is measured with the Hewlett Packard 5245L Electronic Counter. Among the strongest harmonics found in the output of the Frequency Multiplier Chain are those satisfying the relation

$$\text{Output Harmonic} = 10 \times N \times (\text{fundamental frequency})$$

where N is a positive integer. In other words, strong output signals occur at approximately every harmonic of 50 MHz.

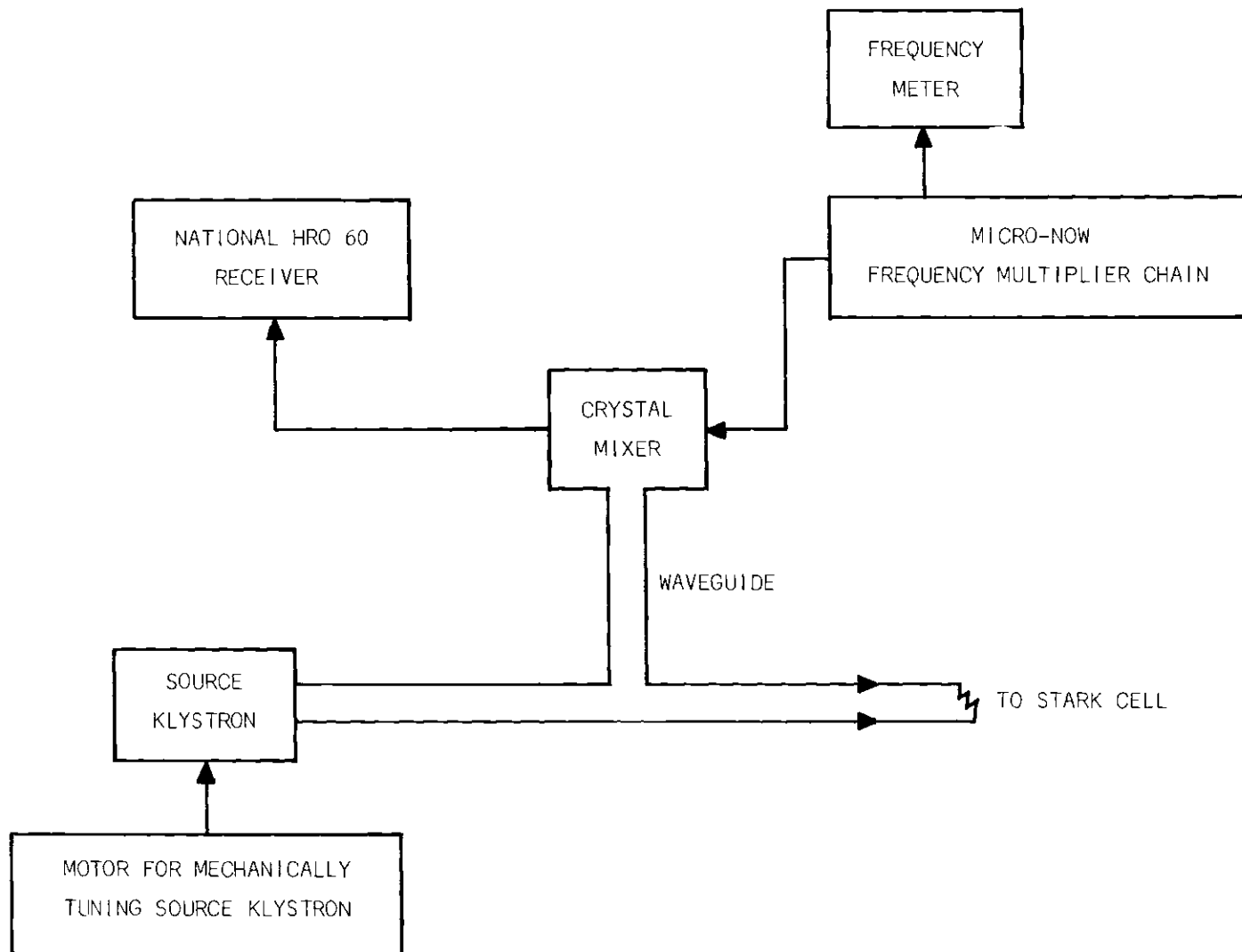


Figure 4. Equipment Set-up for the Beat Note Technique.

Suppose that it is known that the approximate frequency of a Stark component to be measured is 14825 MHz. Suppose further that the fundamental frequency of the Frequency Multiplier Chain has been set at 5.00000 MHz, that the HRO 60 National radio receiver has been set at 24 MHz, and that the klystron is being tuned from approximately 14820 to 14830 MHz. When the klystron frequency reaches 14824 MHz, a 24 MHz beat note is heard in the receiver. This beat note results from the 14824 MHz klystron signal mixing with the 2960th harmonic of the 5.00000 MHz fundamental of the Frequency Multiplier Chain at 14800 MHz.

As the klystron is tuned still further upward in frequency another beat note is heard when the klystron frequency reaches 14826 MHz. This 24 MHz beat note results from the mixing of the klystron signal with the 2970th harmonic of the 5.00000 MHz fundamental of the Frequency Multiplier Chain at 14850 MHz.

If an indication is made on the recording chart whenever a beat note is heard, the chart would have the appearance shown in Figure 5. By ascertaining the position of the center of the Stark component and interpolating, the frequency of the Stark component can be determined.

The precision to which the klystron frequency can be determined is related to the precision to which the fundamental frequency of the Frequency Multiplier Chain can be determined. This measurement in turn depends on the stability of the 1 MHz crystal oscillator in the HP Electronic Counter. As mentioned earlier, the stability of this oscillator is accurate to one part in 10^8 .

Processing the Detector Output

The 30 kHz signal from the crystal detector is connected to several

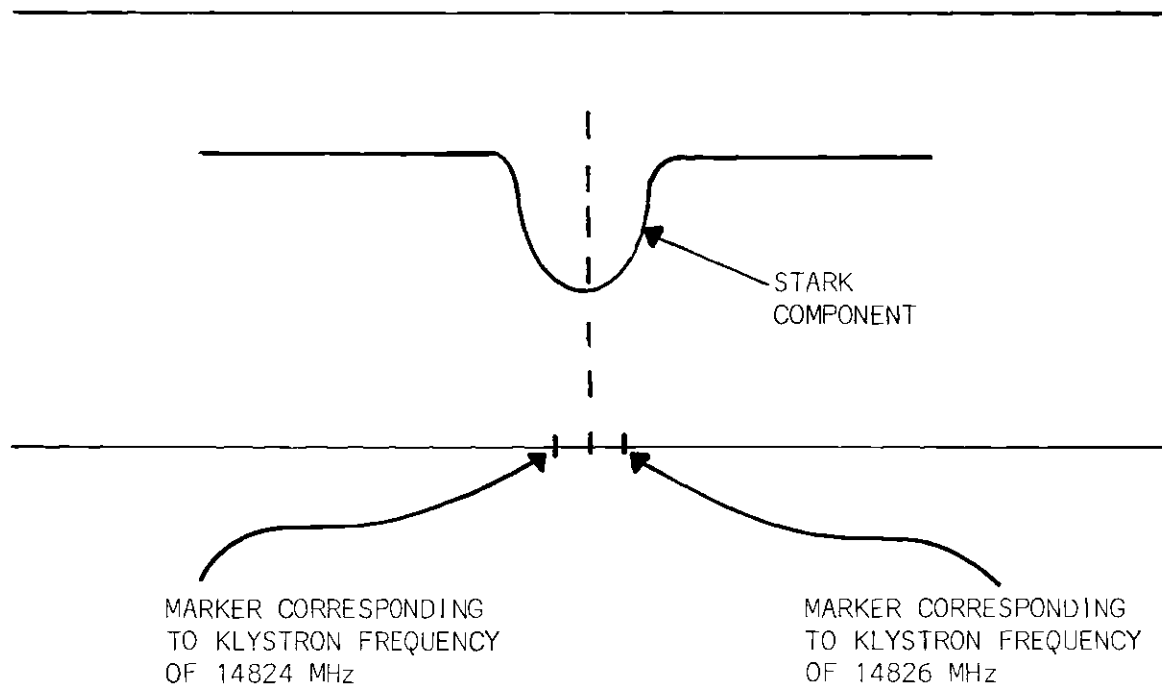


Figure 5. Beat Note Markers on a Recording Chart.

electronic devices as is schematically indicated in Figure 6. The 30 kHz reference signal generated within the PAR Lock-in Amplifier is used to control the frequency and phase of the Stark Field. The situation is indicated in Figure 7 a and b.

If the frequency of the source klystron is such that absorption occurs when the Stark field is on, but not when it is off, then the microwave power fluctuation at the crystal detector is as shown in Figure 7c. After the detector output is fed through the tuned preamplifier, the 30 kHz signal appears as shown in Figure 7d. It should be noted that the signals at a and d are 180° out of phase.

The 30 kHz signal from the preamplifier is fed to the lock-in amplifier, which contains a phase comparator similar to that shown in Figure 1c. Signals a and d of Figure 7 are compared where a is the reference signal.

Referring to Figure 1c, if the preamp signal, E_{preamp} , (labeled E_{if} in the diagram) at b and the reference signal are in phase, then

$$|\vec{E}_{S2}| = |\vec{E}_{\text{ref}} + \vec{E}_{\text{preamp b}}| = |E_{\text{ref}}| + |E_{\text{preamp}}|$$

and

$$|\vec{E}_{S1}| = |\vec{E}_{\text{ref}} + \vec{E}_{\text{preamp a}}| = |E_{\text{ref}}| - |E_{\text{preamp}}|.$$

Thus, $E_o = |E_{S1}| - |E_{S2}| = -2 |E_{\text{preamp}}|.$

This situation is illustrated by the vector diagram of Figure 8a.

By similar reasoning it can be shown that if absorption occurs only when the Stark field is off and not when the field is on, then E_o is a positive voltage as

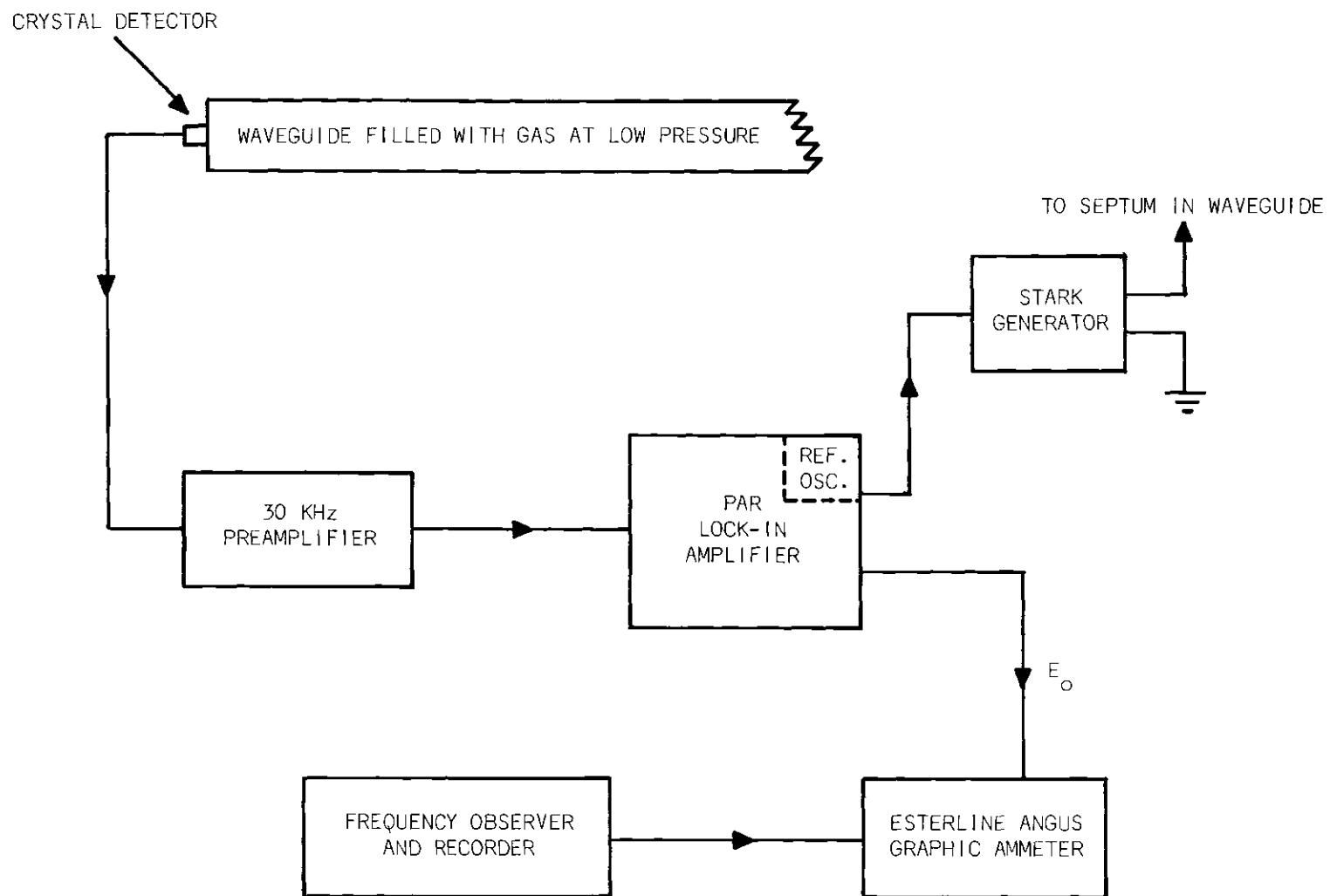


Figure 6. Processing of the 30 KHz Signal from the Crystal Detector.

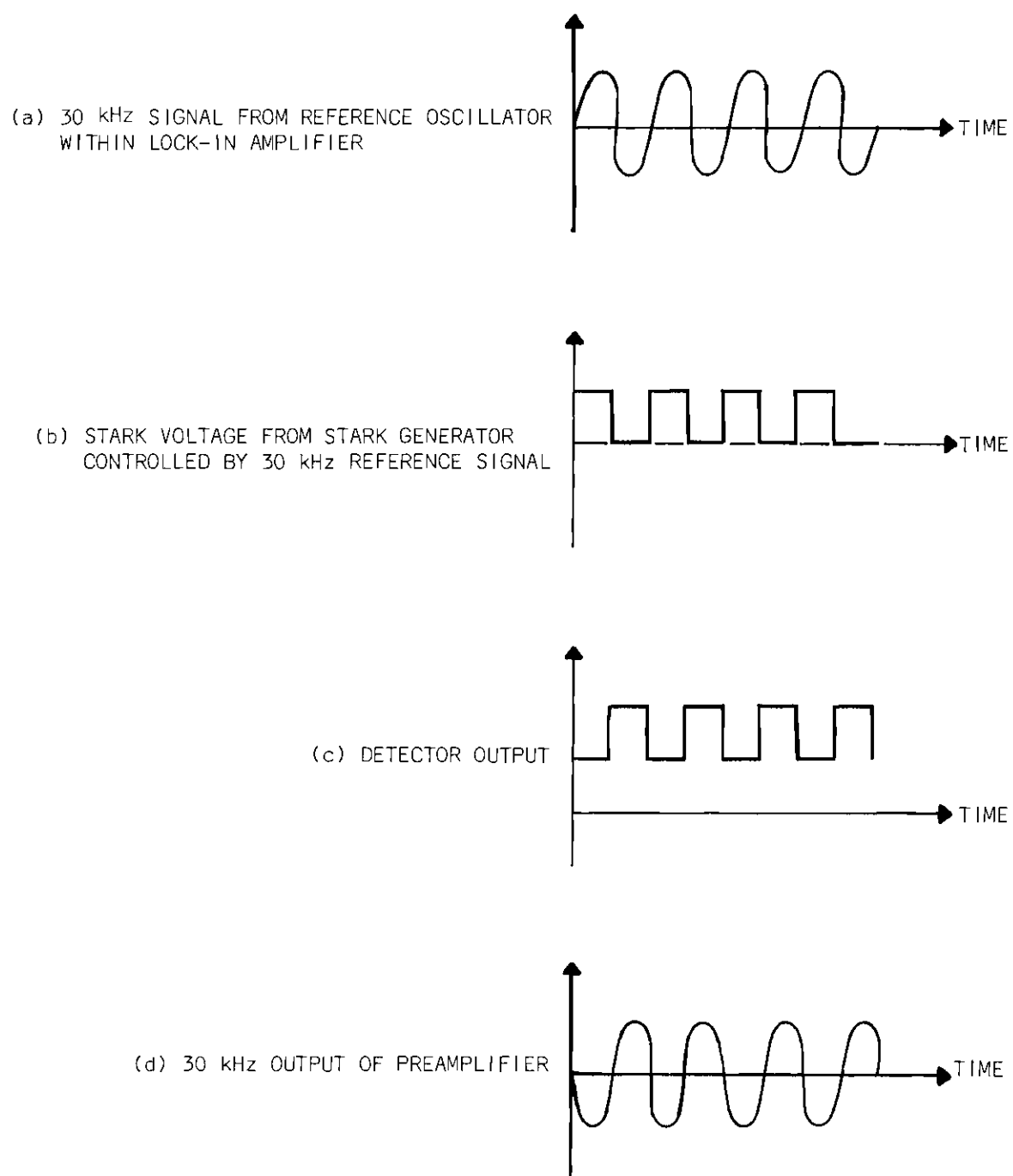
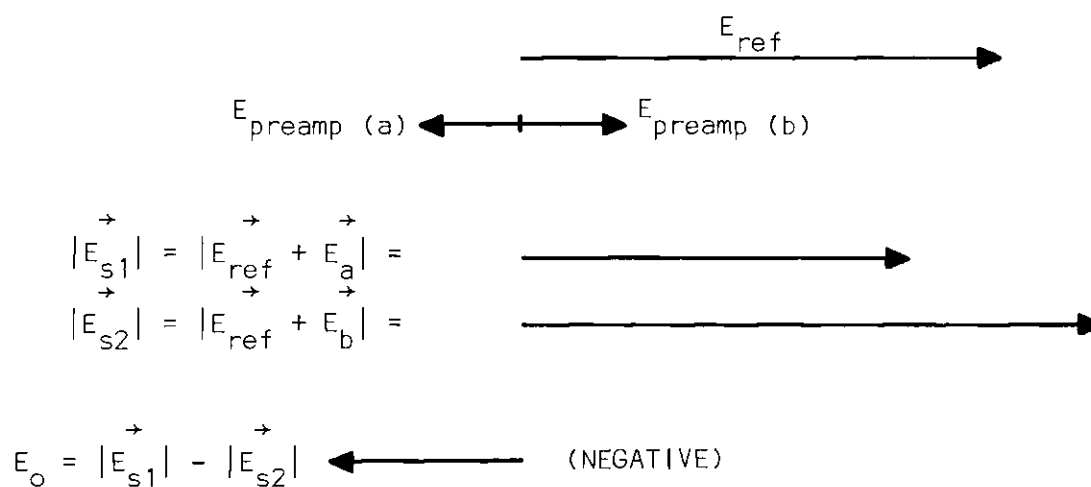
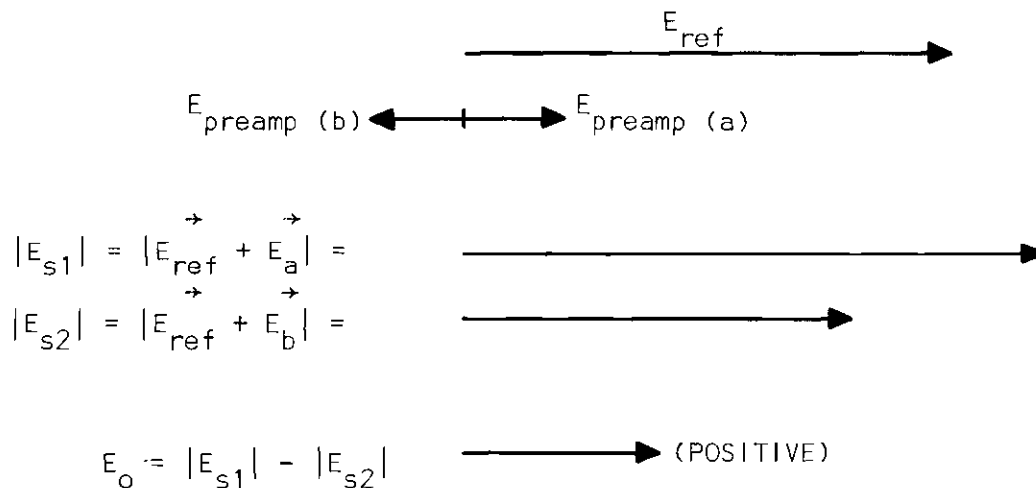


Figure 7. 30 KHz Signals Involved in Processing Detector Output.



(a) ABSORPTION WHEN STARK FIELD IS ON



(b) ABSORPTION WHEN STARK FIELD IS OFF

Figure 8. Vector Diagrams Illustrating Phase Comparator Voltages Under Stark Modulation.

shown in Figure 8b. In general, if absorption occurs both when the Stark field is on and when it is off, then E_0 is proportional to the difference between microwave absorption in absence of Stark field and microwave absorption in presence of Stark field.

In any case, as the source klystron is tuned over the frequency range of interest, E_0 varies between plus and minus values. A plot of E_0 versus source klystron frequency is made by an Esterline Angus Graphic Ammeter. Frequency is measured periodically by making a mark on the recording chart.

Clearly a possible source of error in this process of data taking is the delay in human response between the time the HP Electronic Counter has displayed a count (or a beat note is heard in the HRO 60 receiver) and the time an indication is made on the recording chart. This error is reduced by making runs over the frequency range of interest in pairs: one run going up in frequency, the other going down, and averaging.

Data Gathering Techniques

On either side of the $J = 2$ to 3 rotational lines of CFCl_3 and CHCl_3 are three groups of Stark lines. The frequency separations of these lines from the center of the $J = 2$ to 3 rotational line were measured for several different values of Stark voltage. The technique for measuring the separation was to take the average of 10 runs, 5 up in frequency and 5 down, over the Stark line of interest. As is discussed in Chapter IV, graphs of frequency separation versus Stark field were made for each Stark component measured. These graphs were used to determine dipole moments.

To check theoretically calculated spectra with experimentally measured spectra several runs were made over frequency ranges of interest; a range of frequencies about the rotational line center and extended ranges on either side of the rotational line. These runs and the theoretical calculations are discussed in Chapter IV.

CHAPTER III

THEORY

Quadrupole Interaction Theory

$\text{CF}^{35}\text{Cl}_3$ and $\text{CH}^{35}\text{Cl}_3$ are symmetric top molecules having three identical quadrupolar nuclei each with spin $3/2$. If the quadrupole interaction is ignored, the Hamiltonian operator for the total molecular energy has the form

$$H = H_{\text{el}} + H_{\text{vib}} + H_{\text{rot}},$$

where H_{el} , H_{vib} , and H_{rot} refer to the electronic, vibrational, and rotational energies respectively. The matrix of this Hamiltonian is diagonal in a representation of the form

$$u = \psi_{\text{el}}(\Gamma) \psi_{\text{vib}}(v) \psi_{\text{rot}}(J, K, M),$$

where Γ , v , and J, K, M are appropriate quantum numbers for electronic, vibrational, and rotational states.

If the quadrupole interaction term, H_Q , is added to the Hamiltonian operator above, then a new representation must be found in which to compute the Hamiltonian matrix. It is desirable that this new representation have two important properties: matrix elements are calculable within it, and the basis functions can be classified according to symmetry type under interchange of the identical nuclei. This last property makes it easier to find eigenfunctions which satisfy the Pauli

Exclusion Principle.

After the energy levels and corresponding eigenfunctions have been computed, frequencies and intensities of transitions between energy levels must be determined. In the sections which follow more detailed discussion is given to the form of the quadrupole interaction operator, to the basis functions used in the computation of the Hamiltonian matrix, and to the determination of frequencies and intensities.

The Quadrupole Interaction Operator

The electrostatic interaction between a nucleus and the remainder of electrons and nuclei in an atom or molecule is given by (16)

$$H_{el} = \sum_{ip} \frac{e_i e_p}{|\vec{r}_i - \vec{r}_p|} = + \sum_{ip\ell} \frac{e_i e_p r_p^\ell}{r_i^{\ell+1}} P_\ell(\cos\theta_{ip})$$

where e_p is the charge of the pth proton with position vector \vec{r}_p in the nucleus in question and e_i is the charge of the ith electron or proton with position vector \vec{r}_i in the remainder of the atom or molecule. θ_{ip} is the angle between the vectors \vec{r}_i and \vec{r}_p and P_ℓ is the Legendre function corresponding to the value of ℓ .

The quadrupole interaction term corresponds to $\ell = 2$ in the above series, therefore the quadrupole interaction Hamiltonian is

$$H_Q = \sum_{ip} e_i e_p \frac{r_p^2}{r_i^3} P_2(\cos\theta_{ip}).$$

Using the spherical harmonic addition theorem this interaction operator can be expressed as

$$H_Q = \sum_{ipq} (-1)^q e_i e_p \frac{r_p^2}{r_i^3} C_q^{(2)}(\theta_i, \phi_i) C_{-q}^{(2)}(\theta_p, \phi_p) = (V \cdot Q), \quad (\text{III-1})$$

where

$$V_m^{(2)} = \sum_i \frac{e_i}{r_i^3} C_m^{(2)}(\theta_i, \phi_i),$$

$$Q_m^{(2)} = \sum_p e_p r_p^2 C_m^{(2)}(\theta_p, \phi_p),$$

and the $C_q^{(2)}$ are spherical harmonics of order 2.

This notation and form of expressing the quadrupole interaction operator has been chosen to agree with the notation in the paper by A. A. Wolf (17) and to make apparent the fact that this operator can be expressed as the product of two spherical tensor operators of rank 2. Svidzinski (18) has shown that the total quadrupole interaction operator of three identical quadrupolar nuclei in a symmetric top molecule can be written as three times the interaction energy of one of them. Thus the total quadrupole interaction operator is given by

$$H_Q = 3(V \cdot Q). \quad (\text{III-2})$$

The Hamiltonian Matrix

The set of all functions of the form

$$U = \psi_{el}(\Gamma) \psi_{vib}(v) \psi_{rot}(JKM) \prod_{i=1}^3 u_i(3/2, m_i),$$

where $u_i(3/2, m_i)$ is the nuclear angular momentum eigenfunction of the i th quadrupolar nucleus which has spin $3/2$ and azimuthal quantum number m_i , theoretically

could be used to compute the Hamiltonian matrix. If this set were used matrix elements would be difficult to compute; the matrix would be infinite and probably impossible to diagonalize; and if eigenfunctions could be found, it would be difficult to separate all those that satisfy the Pauli-Exclusion Principle from the rest. Simplification results if certain off-diagonal elements can be ignored and only a finite set of basis functions need be considered; if the basis functions chosen are eigenfunctions of the total angular momentum with quantum number F , and if the basis functions are characterized by definite symmetry type. These concepts are discussed in succeeding paragraphs.

At room temperature and below most CHCl_3 and CFCl_3 molecules are in their lowest electronic and vibrational states. The ground vibrational state is doubly degenerate, and the members of this pair will be identified by the index v which takes on the values 0 and 1. The higher electronic and vibrational levels, and the rotational levels of different J are widely spaced compared to the splitting produced by the quadrupole interaction. Therefore, in the calculation of the interaction energy it is a good approximation to assume that only ground state electronic and vibration eigenfunctions need be considered and that the interaction operator does not link states of different J quantum number.

With this approximation each J level is considered separately and finite matrices result. For the $J = 2$ splittings a complete set of basis functions is the set of 3200 functions of the form

$$U(J=2) = \psi_{\text{el}} (\text{ground state}) \psi_{\text{vib}}(v=0 \text{ or } 1) \psi_{\text{rot}}(2KM) \prod_{i=1}^3 u_i(3/2, m_i).$$

For the $J = 3$ splittings there are 4648 basis functions of the same form but with the J quantum number equal to 3. These functions are more explicitly enumerated in Appendix B.

A More Convenient Representation. In order to take advantage of the Wigner-Eckart Theorem and Racah's algebra of irreducible tensor operators in the calculation of matrix elements, a coupling scheme is chosen in which F , the total angular momentum quantum number ($\vec{F} = \vec{I} + \vec{J}$) is a good quantum number. I is the total spin quantum number ($\vec{I} = \vec{I}_1 + \vec{I}_2 + \vec{I}_3$) of the three quadrupolar nuclei, and γ represents all other appropriate quantum numbers. In this representation the basis functions have the form

$$U(J) = \Psi_{el}(\text{ground state}) \Psi_{vib}(v=0, 1) \Psi_{\text{total ang. mom.}}(F, I, J, \gamma).$$

Several such sets of basis functions can be created. One such set is described below.

Nuclear eigenfunctions characterized by a total nuclear spin, I , can be expressed as linear combinations of various products of individual nuclear spin eigenfunctions,

$$U_{\text{total spin}}(I, M_I) = \sum_{m_1 m_2 m_3} a_{m_1 m_2 m_3} u_1(3/2, m_1) u_2(3/2, m_2) u_3(3/2, m_3), \quad (\text{III-3})$$

where $a_{m_1 m_2 m_3}$ are appropriate coefficients. In fact one possible way to develop such functions is to couple the spins of nuclei 2 and 3 to get an intermediate spin, L , and then couple this spin with the spin of nucleus 1. If this procedure is

followed, the explicit expressions for the resulting eigenfunctions are

$$U_{\text{total spin}}(L, I, M_I) = \sum_{m_1 m_2 m_3 m_L} u_1(3/2, m_1) u_2(3/2, m_2) u_3(3/2, m_3) \cdot (3/2 \ m_2 \ 3/2 \ m_3 | 3/2 \ 3/2 \ L m_L) (3/2 \ m_1 \ L m_L | 3/2 \ L I M_I) \quad (\text{III-4})$$

where the terms $(j_1 m_1 j_2 m_2 | j_1 j_2 j m)$ are vector coupling coefficients.

Basis functions characterized by a given total angular momentum, F , can be constructed by taking appropriate linear combinations of the product of rotational and total nuclear spin eigenfunctions

$$\Psi_{\text{total angular momentum}}(vJK, LI, FM_F) = \sum_{M_I M_J} (IM_I JM_J | IJFM_F) U_{\text{total spin}}(LIM_I) \cdot \Psi_{\text{rot}}(JKM_J) \quad (\text{III-5})$$

where $(IM_I JM_J | IJFM_F)$ are vector coupling coefficients.

A. A. Wolf (19) has shown that in the representation above, the matrix elements of the quadrupole interaction Hamiltonian of nucleus 1 are given by

$$vJK', I', F | H_Q | vJK, I, F) = (-1)^{J+I'+F} \begin{Bmatrix} F & I' & J \\ 2 & J & I \end{Bmatrix} \cdot (vJK' || V || vJK)(I' || Q || I) \quad (\text{III-6})$$

where $\begin{Bmatrix} F & I' & J \\ 2 & J & I \end{Bmatrix}$

is the Wigner six-J symbol of the inclosed quantities. Values for six-J symbols are tabulated in Rotenberg's The 3-J and 6-J Symbols (20). The only values of the reduced matrix elements, $(vJK || V || vJK)$, which will ultimately be needed are (19)

$$(vJK || V || vJK) = \frac{(2J+1) \Gamma 3K^2 - J(J+1)}{[(2J+3)(2J+2)(2J+1)2J(2J-1)]^{1/2}} q \cos \alpha \quad (\text{III-7})$$

and

$$\begin{aligned} (vJ1 || V || vJ-1) &= \frac{(2J+1)J(J+1)q(\cos \alpha - 1)}{2[(2J+3)(2J+2)(2J+1)2J(2J-1)]^{1/2}} \\ &= (vJ-1 || V || vJ1), \end{aligned} \quad (\text{III-8})$$

where α is the Cl-C-Cl angle of the molecule in question and q is the second derivative of the potential with respect to the bond axis, $\frac{d^2V}{dc^2}$. The reduced matrix element, $(3/2, L, I' || Q || 3/2, L, I)$, has been evaluated by Wolf (19) and found to be

$$\begin{aligned} (3/2, L, I' || Q || 3/2, L, I) &= (-1)^{3/2 + L + I + 2} \\ &\cdot [(2I+1)(2I'+1)]^{1/2} \begin{Bmatrix} 3/2 & I & L \\ I & 3/2 & 2 \end{Bmatrix} (3/2 || Q || 3/2). \end{aligned} \quad (\text{III-9})$$

The reduced matrix element, $(3/2 || Q || 3/2)$, has the value, $\sqrt{5}eQ$, where e is the electronic charge, and Q is the quadrupole moment of any one of the identical nuclei.

At this point it is helpful to be aware of two facts. First, if the basis functions of equation III-5 are suitably arranged, the Hamiltonian matrix factors

into a series of non-zero submatrices along its diagonal. Each of these submatrices has elements linking states with the same F , M_F , $|K|$, and J quantum numbers, but not necessarily the same L , K , and I quantum numbers. The situation is depicted in Figure 9.

The second fact is that the sets of basis functions spanning the space of each submatrix are not unique. In the next section, basis functions of each submatrix will be constructed such that their behavior under the interchange of two identical nuclei is known.

Satisfying the Pauli Exclusion Principle. According to the Pauli Exclusion Principle, if any two of the identical fermions (the spin $3/2$ quadrupolar nuclei) are interchanged, the state functions of the Hamiltonian must change sign. That is, acceptable eigenfunctions of the Hamiltonian must change sign under the single interchange of any two identical nuclei. Eigenfunctions exhibiting this kind of behavior are said to have A_2 symmetry type.

If the Hamiltonian of Figure 9 were diagonalized, the resulting eigenfunctions would not necessarily have the appropriate overall symmetry. The problem, then, is to develop for each submatrix a set of basis functions with overall symmetry A_2 .

The first step in the construction of the new set of basis functions is to modify the total nuclear spin functions appearing in equation III-5. The Hamiltonian is unchanged by permutations of the identical nuclei. Therefore, if spin functions are chosen which will serve as basis functions for one of the irreducible representations of the group of permutations of three objects, then there will be

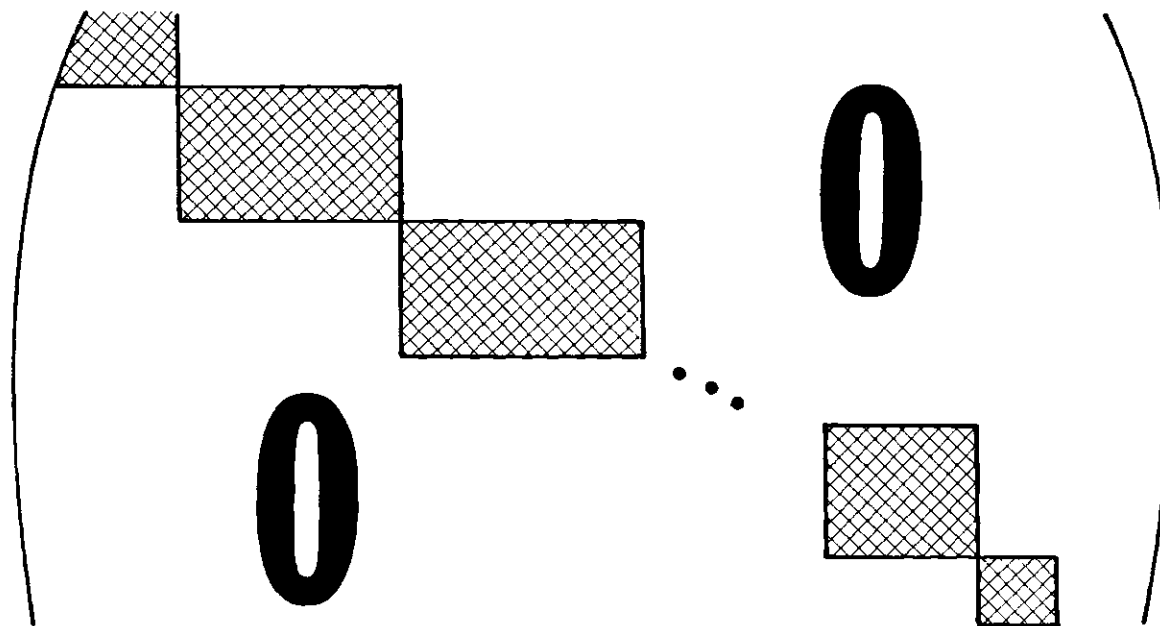


Figure 9. Form of Hamiltonian Matrix in the Representation of Equation III-5.

no matrix elements of the Hamiltonian linking spin functions of different symmetry type (21). Such spin functions have the form

$$U_{\text{total spin}}(w_k, I) = \sum_L G(w_k, L, I) u(L, I) \quad (\text{III-10})$$

where the coefficients, $G(w_k, L, I)$ are called genealogical coefficients. The index, w_k , indicates that the basis functions belong to the w th irreducible representation and behave like the k th row of that representation. In Appendix C, the behavior of basis functions under the action of the group operations is shown for the two one dimensional and the one two dimensional irreducible representations. Values for the genealogical coefficients are also given in Appendix C.

When nuclear spin functions of the form of equation III-10 are used and appropriately arranged in each of the submatrices of the Hamiltonian, then these submatrices divide into smaller submatrices along the diagonal. Each of these smaller submatrices has elements linking only states with nuclear spin functions of the same symmetry. The situation is shown in Figure 10.

At this point a typical basis function has the form

$$\begin{aligned} \Psi(vJK, w_k, I, FM_F) &= \Psi_{\text{el}}(\text{ground state}) \Psi_{\text{vib}}(v=0 \text{ or } 1) \\ &\cdot \sum_{M_I M_J} (IM_I JM_J | IJFM_F) u_{\text{total spin}}(I, M_I, w_k) \Psi_{\text{rot}}(J, K, M_J) \end{aligned} \quad (\text{III-11})$$

and the general expression for a matrix element is (22)

$$(vJK', w_k, I', F | 3H_Q | vJK, w_k, I, F) = (-1)^{J+I'+F} \quad (\text{III-12})$$

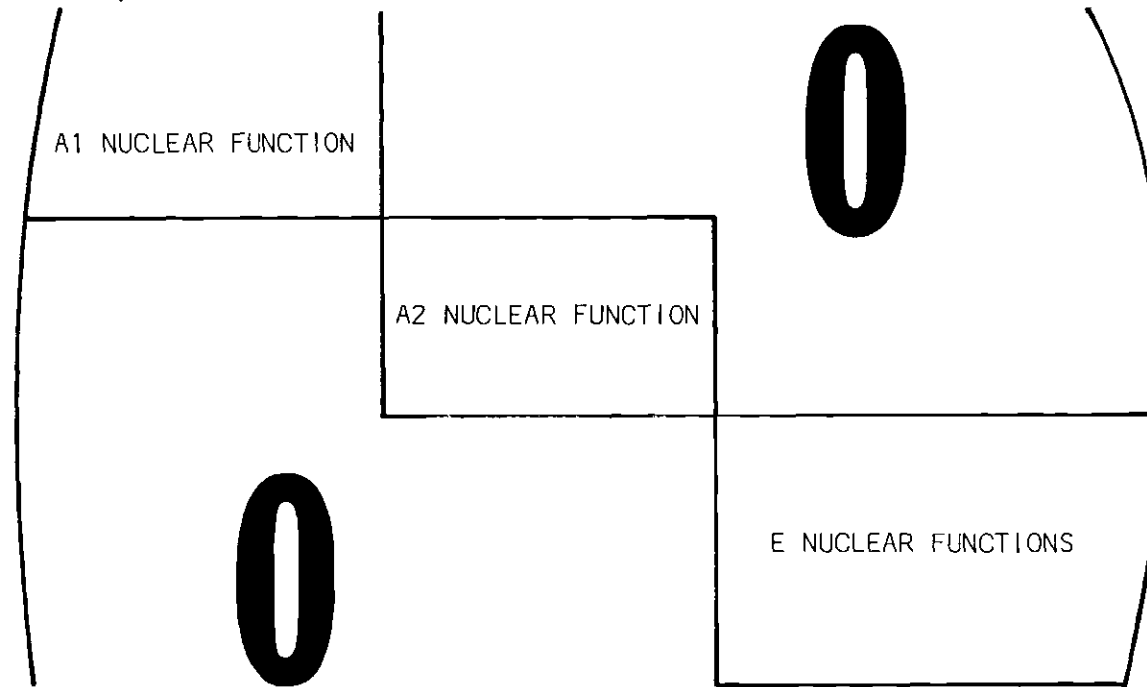


Figure 10. The Form of a Typical Submatrix when Spin Functions, $u(w_k I)$, are used.

$$\begin{aligned}
& \cdot \left\{ \begin{matrix} F & I' & J \\ 2 & J & I \end{matrix} \right\} (vJK' \| V \| vJK) (3/2 \| Q \| 3/2 [(2I+1)(2I'+1)])^{1/2} \\
& \sum_L \left[(-1)^{3/2+L+I'} G(w_k, L, I) \left\{ \begin{matrix} 3/2 & I' & L \\ I & 3/2 & 2 \end{matrix} \right\} G(w_k, L, I) \right] .
\end{aligned}$$

Since further modifications to the sets of basis functions are still needed, and the notation is already cumbersome, it is convenient to collect those terms involving only spin quantum numbers and define a nuclear reduction coefficient by

$$C(w_k, I', I) = 3(-1)^{I'+I} [(2I+1)(2I'+1)]^{1/2} \quad (\text{III-13})$$

$$\sum_L \left[(-1)^L G(w_k, L', I') \left\{ \begin{matrix} 3/2 & I' & L' \\ I & 3/2 & 2 \end{matrix} \right\} G(w_k, L', I) \right] .$$

In Appendix C are listed the reduction coefficients needed for the $J = 1$ to 2 , $K = 1$ and the $J = 2$ to 3 , $K = 1, 2$ calculations. Substituting equation III-13 into III-12 one gets

$$\begin{aligned}
(vJK' \| w_k I', F | 3H_Q | vJK, w_k I, F) &= (-1)^{3/2+J+F} \left\{ \begin{matrix} F & I' & J \\ 2 & J & I \end{matrix} \right\} \\
(vJK' \| V \| vJK) (3/2 \| Q \| 3/2) C(w_k, I', I).
\end{aligned} \quad (\text{III-14})$$

If any of the submatrices indicated in Figure 10 is diagonalized, the resultant eigenfunctions, which are linear combinations of basis functions, would be characterized by the symmetry of only the nuclear spin part of the wavefunctions. However, what is needed is a method by which eigenfunctions of overall A_2 symmetry can be found.

Consider any one of the submatrices of nuclear spin symmetry, A1, A2, or E shown in Figure 10. Each of these submatrices is spanned by a set of basis functions of the form indicated in equation III-11. However, it is more convenient to span the spaces of these submatrices with functions which are certain linear combinations of the functions in equation III-11. Some of these linear combinations will result in basis functions with A2 overall symmetry (23) - viz.

1. In an A1 or A2 submatrix if the quantum number, K, is equal to zero or an integral multiple of three, then basis functions of the form

$$\Psi(v, E_{JK}, A_{1,2}, I, F) = 1/\sqrt{2} [\Psi(vJK, A_{1,2}, I, F) \mp (-1)^{J+V} \Psi(vJ-K, A_{1,2}, I, F)] \quad (\text{III-15})$$

$$\Psi(vJ-K, A_{1,2}, I, F)]$$

have A2 overall symmetry, where the - sign is used for an A1 submatrix and the + sign is used for an A2 submatrix.

2. In any E submatrix if K is not zero and not an integral multiple of three, then basis functions of the form

$$\Psi(v, E_{JK}, E, I, F) = 1/2 [\Psi(vJK, E_2, I, F) - (-1)^{J+V} \Psi(vJ-K, E_2, I, F)] + i/2 [\Psi(vJK, E_1, I, F) + (-1)^{J+V} \Psi(vJ-K, E_1, I, F)] \quad (\text{III-16})$$

$$+ i/2 [\Psi(vJK, E_1, I, F) + (-1)^{J+V} \Psi(vJ-K, E_1, I, F)]$$

$$\Psi(vJ-K, E_1, I, F)]$$

have A2 overall symmetry.

3. No other linear combinations of the functions of the form of III-11 yield basis functions having overall A2 symmetry.

There are no non-zero matrix elements linking states of A2 overall symmetry with states of non-A2 overall symmetry (21). Therefore, one can group the matrix elements linking basis functions of A2 overall symmetry into still smaller submatrices and diagonalize these submatrices. The eigenfunctions of these submatrices will then have A2 overall symmetry.

Thus, the Pauli Exclusion Principle is satisfied by only accepting those eigenfunctions resulting from the diagonalization of an A2 (overall) submatrix.

Transition Frequencies and Intensities

The relative intensity of a rotational transition in a molecule is proportional to the square of the matrix element of the electric dipole moment operator between initial and final states. When the matrices of the quadrupole interaction are diagonalized the state function corresponding to a hyperfine level is given by Wolf (24) in the following form

$$u(E_{JK}^T) = \sum_I B_{TI} u(E_{JK}^{wIF M_F}),$$

where the quantities, B_{TI} , are the matrix elements of the diagonalizing transformation. The index T is used to distinguish states corresponding to different eigenvalues.

Choosing the space fixed axis to be in the direction of the electric field, noting that the dipole moments of CFCl_3 and CHCl_3 lie along their molecular axes, and using the Wigner-Eckart theorem and Racah's algebra of irreducible tensor

operators, A. A. Wolf gets the expression

$$N = \left[\frac{(J+1)^2 - K^2}{3(J+1)} \right] d^2 (2F^i+1)(2F^f+1) \left[\sum_I B_{TI} B_T (-1)^{J+I+F^f+1} \begin{Bmatrix} J^i & F^i & I \\ F^f & J^f & 1 \end{Bmatrix} \right]^2 \quad (\text{III-17})$$

for the relative intensity of the transition between a $J = 2$ hyperfine level and a $J = 3$ hyperfine level. In this expression d is the dipole moment. The frequency of any such line is given by

$$\begin{aligned} \text{Frequency} = & [\text{Freq. of rotational transition}] + [J = 3 \text{ HFS}] \\ & - [J = 2 \text{ HFS}] , \end{aligned}$$

where $[J = 3 \text{ HFS}]$ is the hyperfine splitting of the $J = 3$ level.

A. A. Wolf further notes that for the case $J = 3$, $K = 2$ the reduced matrix element $(vJK \parallel V \parallel vJK)$ vanishes so that all of the quadrupole hyperfine levels are degenerate. "The intensities of the lines involving these levels were computed using $B_{TI} = 1$ for each value of I , calculating the intensities corresponding to different values of I separately, and adding all of the intensities corresponding to the same frequency." (25)

The Combined Stark and Quadrupole Interaction

The Hamiltonian operator for the combined Stark and quadrupole interactions has the form,

$$H_{Q+S} = H_Q + H_S,$$

where H_Q is the quadrupole interaction operator discussed in the preceding

section, and H_S is the Stark interaction operator. The Stark interaction operator can be written in the spherical tensor notation of Edmonds (16) as

$$H_S = \sum_{\mu} (-1)^{\mu} d_{\mu}^{(1)} E_{-\mu},$$

where μ can take on the values -1, 0, 1. E refers to the applied electric field and d to the electric dipole moment of the molecule. In terms of cartesian components, the spherical components of these quantities are given by

$$\begin{aligned} d_1^{(1)} &= \frac{-1}{\sqrt{2}} (d_x^{(1)} + i d_y^{(1)}) & E_{-1} &= + \frac{1}{\sqrt{2}} (E_x - i E_y) \\ d_0^{(1)} &= d_z^{(1)} & E_0 &= E_z \\ d_{-1}^{(1)} &= \frac{+1}{\sqrt{2}} (d_x^{(1)} - i d_y^{(1)}) & E_1 &= \frac{-1}{\sqrt{2}} (E_x + i E_y). \end{aligned}$$

The representation used to compute the quadruple interaction Hamiltonian matrix is also used to compute the combined Stark and quadrupole Hamiltonian matrix, therefore a typical matrix element has the form

$$\langle v' J' K' w_k' I' M_F' | H_{Q+S} | v J K w_k I M_F \rangle = (\dots | H_e | \dots) + (\dots | H_S | \dots). \quad (\text{III-19})$$

Before discussing the evaluation of the terms on the right, it is helpful to look at the overall form of the Hamiltonian matrix. Since neither the quadrupole interaction operator nor the Stark interaction operator links states having different M_F quantum numbers, a suitable arrangement of matrix elements results in a matrix

of the form shown in Figure 11 -- that is, a series of submatrices strung along the diagonal. Each of the submatrices has elements which link states of the same M_F quantum number. Further arrangement of matrix elements within each submatrix can result in a Hamiltonian matrix having the form shown in Figure 12 -- that is, each submatrix is further subdivided into two matrices, one of which is characterized by the fact that it links only states of A2 overall symmetry.

As in the quadrupole case, eigenfunctions having the required A2 symmetry result from diagonalizing only the A2 submatrices.

Equations III-14 and III-16 enable one to evaluate the quadrupole terms. It should be noted that these terms only link states for which $F' = F$ and $v' = v$.

Using the Wigner-Eckart theorem and appropriate equations from Edmonds, C. R. Nave (26) has derived an expression for the Stark term

$$\begin{aligned}
 (vJK, wI, FM_F | H_S | v'JK, wI, F'M_F) &= (2J+1)(-1)^{F+F'-M_F+I-K+1} \\
 & \left[(2F+1)(1F'+1) \right]^{1/2} \begin{pmatrix} F & 1 & F' \\ -M_F & 0 & M_F \end{pmatrix} \begin{pmatrix} J & 1 & J \\ K & 0 & -K \end{pmatrix} \left\{ \begin{matrix} J & F & I \\ F' & J & 1 \end{matrix} \right\} \text{Ed.} \quad (\text{III-20})
 \end{aligned}$$

The expressions,

$$\begin{pmatrix} F & 1 & F' \\ -M_F & 0 & M_F \end{pmatrix}$$

and

$$\begin{pmatrix} J & 1 & J \\ K & 0 & -K \end{pmatrix}$$

are 3-J symbols of the inclosed quantities. Values for 3-J symbols have been tabulated by Rotenberg (20). Only terms for which $v' = v \pm 1$ are non-zero. Note

$$\begin{pmatrix}
 M_F = 11/2 & & & & \\
 & M_F = 9/2 & & & \\
 & & \ddots & & \\
 & & & \ddots & \\
 & & & & \ddots
 \end{pmatrix}
 \begin{pmatrix}
 0 \\
 \\
 \\
 \\
 \\
 \end{pmatrix}$$

Figure 11. Form of Hamiltonian Matrix for Combined Stark and Quadrupole Interaction.

A2 $M_F = 11/2$	0		
0	NON A2 $M_F = 11/2$		
		A2 $M_F = 9/2$	0
		0	NON A2 $M_F = 9/2$
		...	

Figure 12. Form of Hamiltonian Matrix for Combined Stark and Quadrupole Interaction when Basis Functions are Symmetrized.

however that due to properties of the 3-J symbol, non-zero elements result for $F' - F = 0, \pm 1$ only. Non-zero matrix elements linking states of different J are ignored. This approximation is reasonable since the Stark splittings for the electric field strengths of interest are small compared to the rotational energy level separations.

The transition frequencies are given by

$$\begin{aligned} \text{Frequency} = & [\text{unperturbed rotational transition frequency}] \\ & + [J = 3 \text{ splitting}] - [J = 2 \text{ splitting}]. \end{aligned} \quad (\text{III-21})$$

The intensity of a transition between two eigenstates is proportional to the square of the matrix element of the dipole moment operator linking the two states.

C. R. Nave (27) has derived the following expression for the intensity of a transition between eigenstates characterized by the symbols f_1 and f_2 :

$$I = \left[\sum_{\substack{I, F, F', \\ v \neq v'}} (vJKIFM_F | f_1) (v'J'KIF'M_F' | f_2) \cdot (vJKIFM_F | d^{(1)} | v'J'KIF'M_F') \right]^2$$

where $(vJKIFM_F | d^{(1)} | v'J'KIF'M_F')$ is given by equation III-20 if the E is dropped from that equation. Equation III-22 holds for the case where the microwave field is parallel to the Stark field.

Stark Effect in the Absence of Quadrupole Splitting

If the Stark field is sufficiently strong, then the Stark interaction term in equation III-19 is much larger than the quadrupole interaction term, and to

a good approximation one can ignore the quadrupole term entirely. C. R. Nave (13) has shown that the expression for the magnitude of the Stark splittings on either side of a rotational transition for the case where the quadrupole interaction is ignored,

$$\Delta \nu = \frac{2M_J K \mu V}{J(J+1)(J+2)d} \left(\frac{0.50348 \text{ MHz}}{\text{debye volt/cm}} \right), \quad (\text{III-23})$$

can be applied in the case where the Stark interaction is much stronger than the quadrupole interaction. In this expression, V is the stark voltage, d is the separation between the Stark electrode and the waveguide walls, J is the rotational quantum number of the lower level, and μ is the dipole moment.

For the $J = 2$ to 3 transition the values that $M_J K$ can have in equation III-23 are one, two, and four. The intensity of any of these splitting is proportional to the square of the matrix element of dipole moment operator linking the initial and final states. Using expressions for dipole moment matrix elements from Townes and Schawlow (28), one obtains the following expression for the square of the dipole moment matrix element,

$$(J+1, K, M_J | \mu_{\text{operator}} | J, K, M_J)^2 = \frac{\mu^2 [(J+1)^2 - K^2] [(J+1)^2 - M_J^2]}{(J+1)^2 (2J+1)(2J+3)} \quad (\text{III-24})$$

Thus, 64:80:25 is the ratio of intensities for the Stark components corresponding to $M_J K$ equaling one, two, and four respectively.

As is discussed in Chapter IV, equation III-23 is used in the determination of the dipole moments of CHCl_3 and CFCl_3 .

Pressure Broadening

Of all the factors contributing to the broadening of spectral lines, the largest by far is pressure broadening (29). At low pressures and over a 5 to 10 MHz region about a rotational line, the Van Vleck and Weisskopf pressure broadening equation can be approximated by

$$\gamma = \frac{Cbp}{(\nu - \nu_0)^2 + (bp)^2}, \quad (\text{III-25})$$

where

C is a constant

b is the line width parameter

p is the gas pressure

ν_0 is the natural molecular frequency

γ is the absorption coefficient.

The line width parameter, b, can be determined from the equation

$$\Delta \nu = 2 bp$$

where $\Delta \nu$ is the width of the line at half-maximum (30).

When making theoretical calculations which are to be compared with actual recordings of data, one must take pressure broadening effects into account, since an overlap of lines can affect the spectrum appearance.

CHAPTER IV

ANALYSIS OF DATA

In order to facilitate the analysis and interpretation of data, several computer programs were written in the course of this research:

1. **BESTFIT** a program to determine the slope and y-intercept of the best (Least Squares) straight line fit to a series of points, (x_i, y_i) . This program was used in the determination of dipole moments for CHCl_3 and CFCl_3 .
2. **KISZERO** a program which computes the frequencies and intensities of all $J = 2$ to 3 , $K = 0$ quadrupole transitions. This program also computes a pressure broadened spectrum over any specified frequency range of interest.
3. **KONETWO** a program which computes the frequencies and intensities of all $J = 2$ to 3 , $K = 1, 2$ quadrupole transitions. This program also computes a pressure broadened spectrum over any specified frequency range of interest.
4. **PBRTAPE** a program which computes a. the frequencies and intensities of all $J = 2$ to 3 , $K = 1, 2$ quadrupole transitions and b. the frequencies and intensities of all $J = 2$ to 3 , $K = 1, 2$ combined Stark and quadrupole transitions. This program also computes 3 pressure broadened spectra over any specified frequency range of interest:

a. a quadrupole spectrum, b. a combined Stark and quadrupole spectrum, and c. a difference spectrum resulting from spectrum "a" being subtracted from spectrum "b". One of the options of this program causes a tape to be made of all computed frequencies and intensities.

5. PBRTTEST a program which computes several pressure broadened spectra corresponding to different values of pressure and line width parameter in equation III-25. Input data to this program consists of the tape information computed by PBRTAPE and data cards containing the values of pressure and line width parameter for which pressure broadened spectra are to be computed.

Of these programs, PBRTAPE was by far the most useful and indispensable to the research. A printout of this program is included in Appendix D. The logic and operation of this program are discussed in Appendix E.

PBRTAPE takes between one and one and a half hours of computer time (Processor and IO) to run and thus from this fact alone one can see how handicapped the research would have been without this program or its equivalent.

In the sections which follow, theoretical calculations are compared with experimental measurements.

Electric Dipole Moment Determinations

Equation III-23 for the frequency separation of Stark components from a main rotational line becomes

$$\Delta \nu = 0.04196 (M_J K) \mu E \quad (\text{IV-1})$$

for the $J = 2$ to 3 rotational transition. $\Delta \nu$ is the frequency separation in MHz; μ is the electric dipole moment of the molecule in debyes; and E is the strength of the Stark electric field in volts/cm. Since the quantity $M_J K$ can take on the values one, two, and four for this transition, a graph of frequency separation plotted against Stark field consists of three straight lines passing through the origin.

The dipole moment of a given molecule is related to the slope of any of these lines by the following relation:

$$\mu \text{ (in debyes)} = \frac{\text{slope (in MHz/volt/cm)}}{0.04196 (M_J K)} \quad (\text{IV-2})$$

As mentioned in Chapter II, frequency separations of the Stark components from the $J = 2$ to 3 rotational line in CHCl_3 and CFCl_3 were measured for several different values of the Stark electric field. These frequency separations are plotted against the field strength in Figures 13 and 14 for CHCl_3 and CFCl_3 respectively. These measurements were made using the double phase-lock stabilization technique.

For both molecules, the measurements made on the Stark component corresponding to $M_J K$ equal to two were the most reliable. That Stark component is the most intense of the three. Therefore, dipole moment determinations were based on measurements made on that component.

A Least Squares fitting technique was used to find the best straight line fit to the $M_J K$ equal to two component for each molecule. From the slopes of these lines, the molecular dipole moments of the molecules were determined. In order to have some measure of the reliability of results, the 90 per-cent confidence

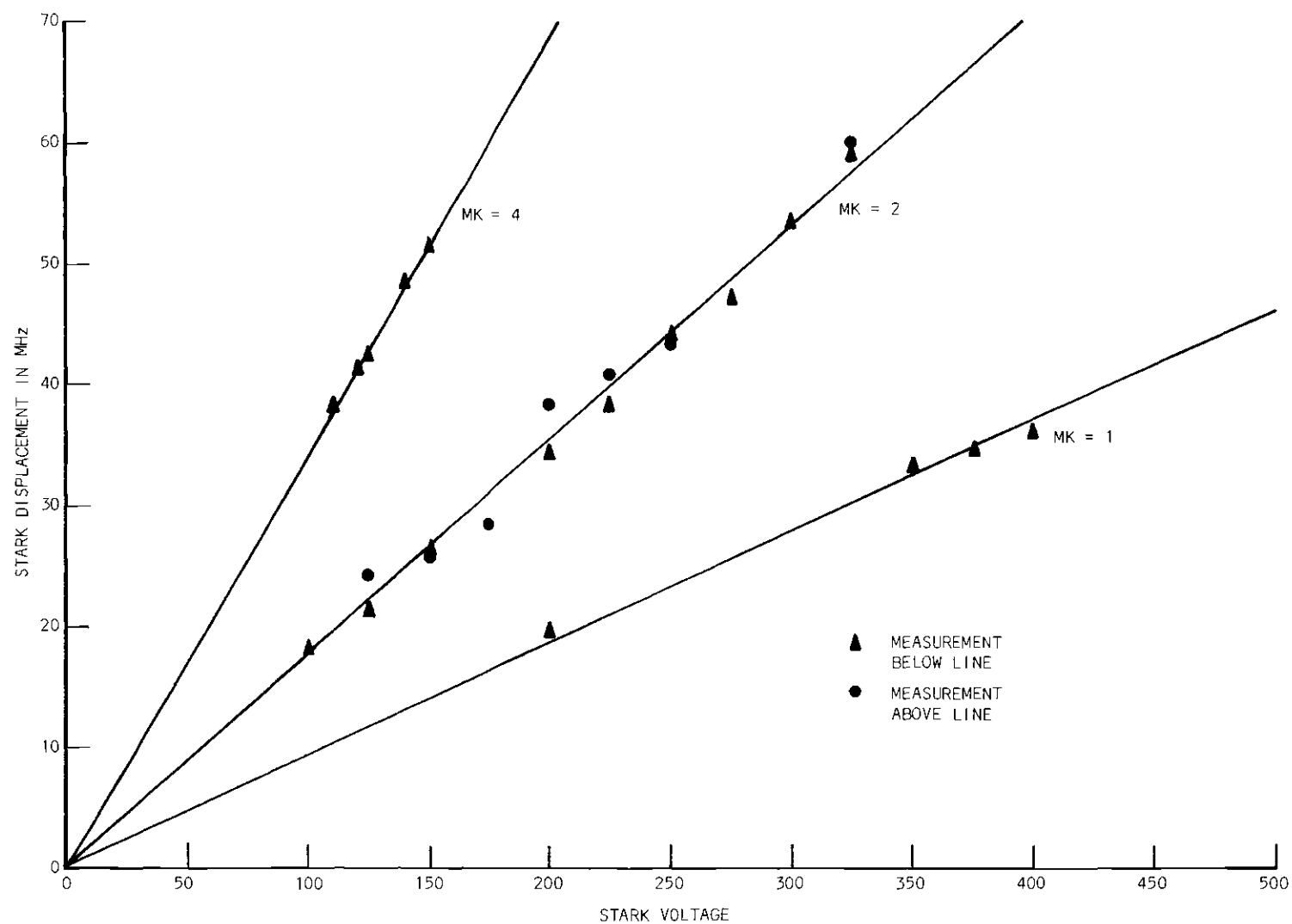


Figure 13. Stark Components of CHCl_3 Measured by Double Phase Lock Stabilization Method.

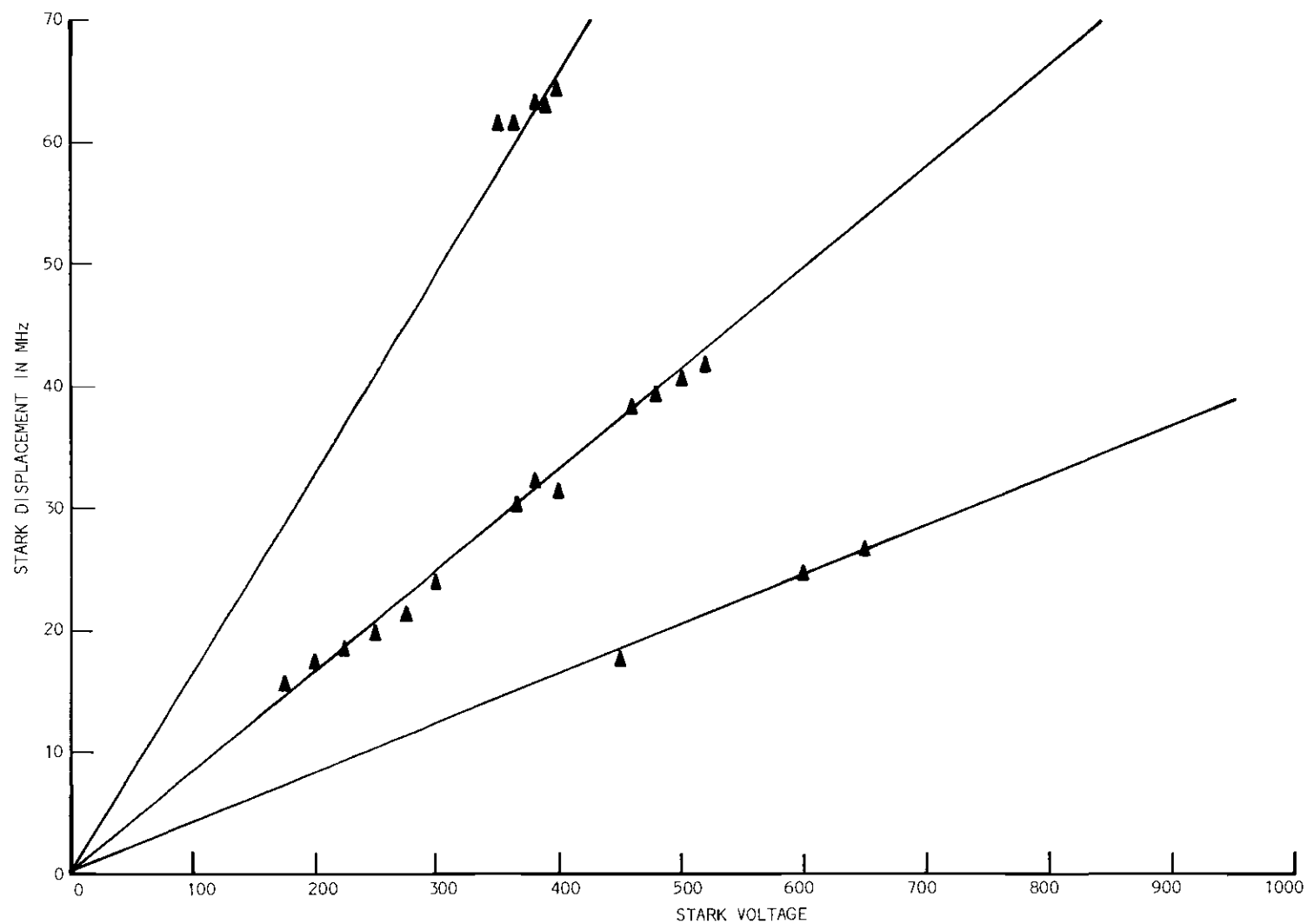


Figure 14. Stark Components of CFCl_3 Measured by Double Phase Lock Stabilization Method.

intervals for each of these slopes was computed. These intervals were calculated as follows:

1. In a student's T-table (found in any standard book of statistical tables) the appropriate t-value was determined for the line in question (The appropriate t-value is the one corresponding to (N-2) degrees of freedom, where N is the number of measured points on the line.),
2. The standard deviation of the slope, S_b , was computed using the equation

$$S_b = \sqrt{\frac{\sum_i (y_i - \bar{y})^2}{(N-2) \sum_i (x_i - \bar{x})^2}}$$

- and 3. The 90 per-cent confidence interval in the slope was calculated as the product, $S_b t$.

Since the measurements made on CHCl_3 using the double phase-lock stabilization technique yielded points widely scattered from the straight line of best fit, it was decided to repeat the dipole moment determinations for both CHCl_3 and CFCl_3 using the beat note technique. Figures 15 and 16 are plots of the frequency separation of the second Stark component versus electric field for CHCl_3 and CFCl_3 respectively, using this technique.

In Table 1, the author's measured values for the dipole moments of CHCl_3 and CFCl_3 are compared with values obtained by other researchers. The author's results are stated at the 90 per-cent confidence level.

Comparison of Observed with Calculated Spectra

Using the pressure broadening formula, III-25, several pressure broadened

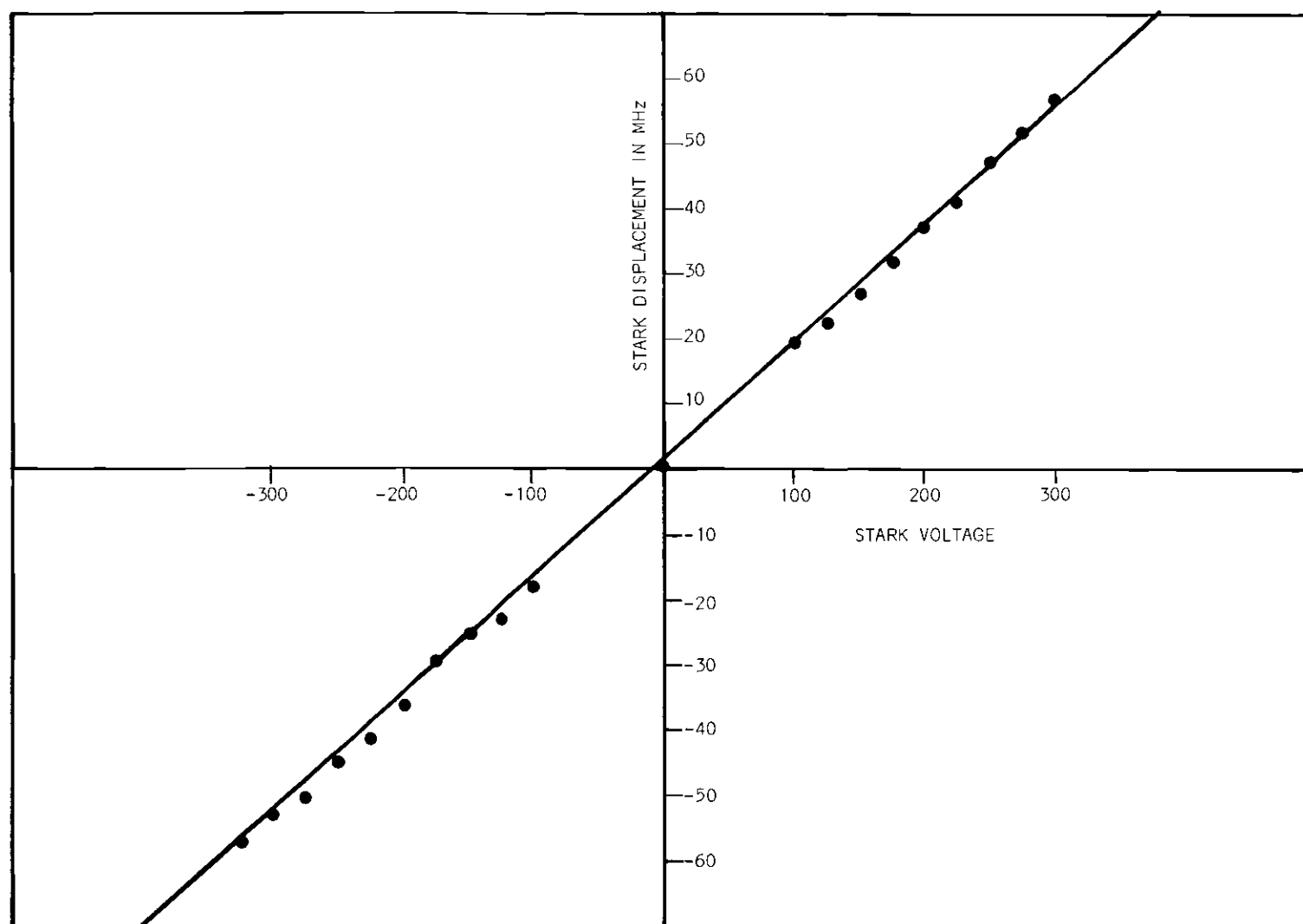


Figure 15. Second Stark Components of CHCl_3 Measured by Beat Note Method.

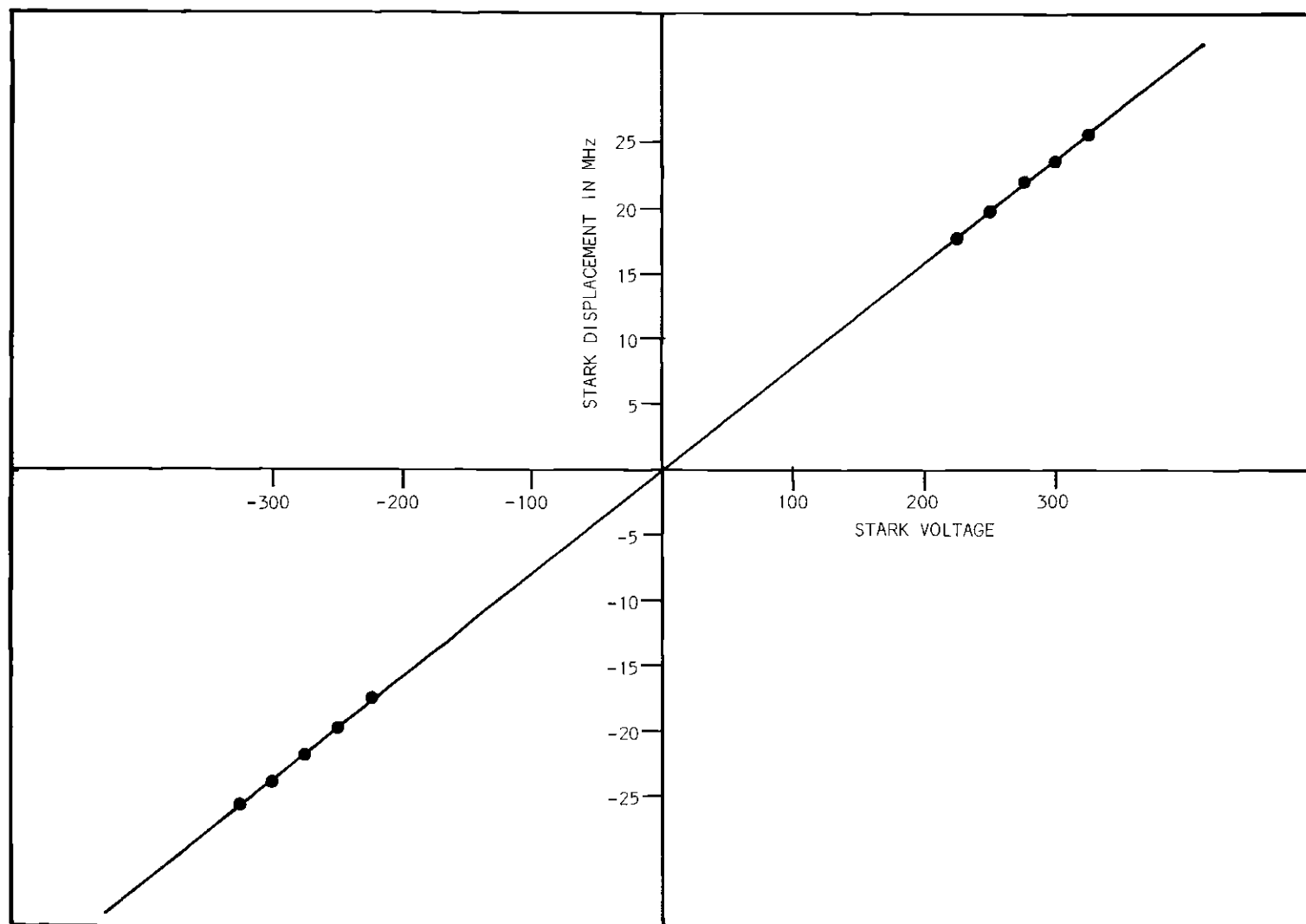


Figure 16. Second Stark Components of CFCl_3 Measured by Beat Note Method.

Table 1. Electric Dipole Moment Measurements of
 CHCl_3 and CFCl_3 in the Gaseous State

Molecule	μ in debye	Method	Researcher and Reference
CHCl_3	0.9	Dielectric constant	Sanger, R., Physik, z. <u>27</u> , 556-63 (1926).
	1.00 ± 0.01	Dielectric virial coefficient	Buckingham, A.D., and Raab, R. E., J. Chem. Soc., 5511-23 (1961).
	1.03	Dielectric constant	Ramaswamy, K. L., Proc. Indian Sci. <u>2A</u> , 364-77 (1935).
	1.06	Dielectric constant	Sircar, S. C., Indian J. Phys. <u>3</u> , 197-208 (1928).
	1.07	Dielectric constant	LeFevre, R. J., Wand, Russell P., J. Chem. Soc., 491-5 (1936).
	1.86	Dielectric constant	Maryott, A. A., Hobbs, M. E., and Gross, P. M., J. Am. Chem. Soc. <u>62</u> , 2320-4 (1940).
	1.025 ± 0.04	Stark Effect	Present work, Method 1
	1.04 ± 0.01		Present work, Method 2
CFCl_3	0.45 ± 0.01	Dielectric constant	Roberti, D. M., Kalman, O. F. & Symth, C. P., J. Amer. Chem. Soc. <u>82</u> , 3523-6 (1960).
	0.53	Dielectric constant	Fuoss, R. M., J. Amer. Chem. Soc. <u>60</u> , 1633-7 (1938).
	0.46 ± 0.02	Stark Effect	Present work, Method 1
	0.46 ± 0.02	Stark Effect	Present work, Method 2

spectra for CHCl_3 were computed for different values of the product, bp . Four of these spectra are reproduced in Figures 17 through 20 corresponding to the product, bp , having values 0.25, 0.50, 0.75, and 1.0 MHz respectively. Figure 21 is a reproduction of the spectrum of CHCl_3 made under conditions similar to those for which the computed spectra were calculated.

Three observations are made in comparing the calculated and measured spectra. First, the calculated spectrum corresponding to $bp = 0.5$ MHz resembles the measured spectrum most closely. Second, the calculated spectra indicate the great effect pressure broadening can have on the appearance of spectral lines. For example, in Figure 17, line A is more intense than lines B and C. In Figures 18-20 these relative intensities are reversed. Further, as the pressure broadening effect is increased the spectral lines lose their distinctiveness.

The third observation is that the computed spectra more closely resemble measured spectra below the rotational line center than above. Although the exact reason for this discrepancy is not known, several possible contributing factors can be listed: 1. The calculated spectrum is made for the molecule in its ground vibrational state, but included in the measured spectrum are weaker spectra due to excited states that can exist. 2. The strength of the measured spectrum is very close to the sensitivity limits of the microwave spectrograph, and background noise may not be of a random nature. 3. The $K = 0$ lines whose contribution is not taken into account in the calculated spectrum may have more than the expected negligible effect on the spectrum.

The calculated spectrum of CFCl_3 for $bp = 0.25$ MHz is shown in Figure 22 and the measured spectrum is shown in Figure 23.

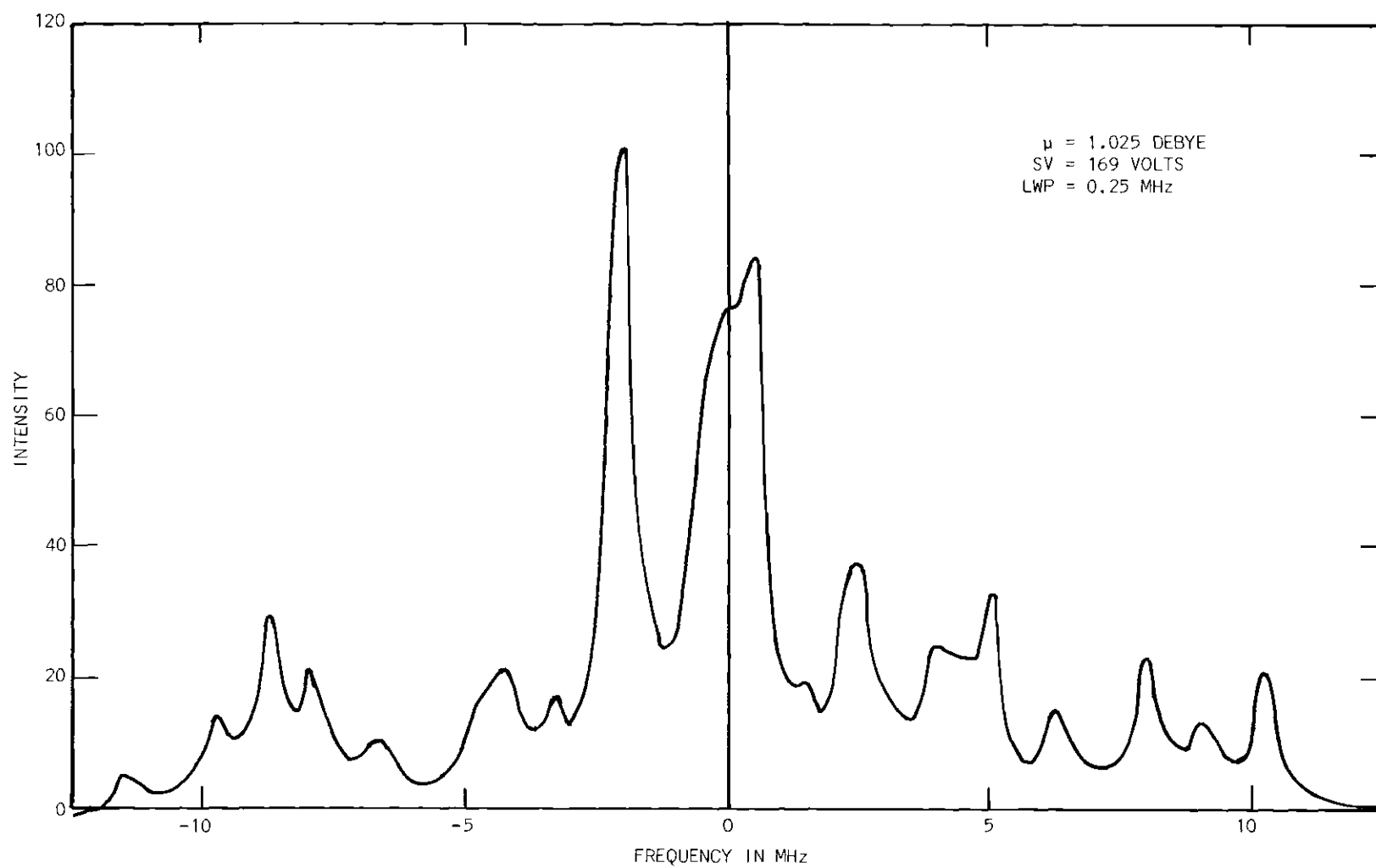


Figure 17. Calculated Pressure Broadened Spectrum for the
 $J = 2 - 3$ Transition of CHCl_3 .

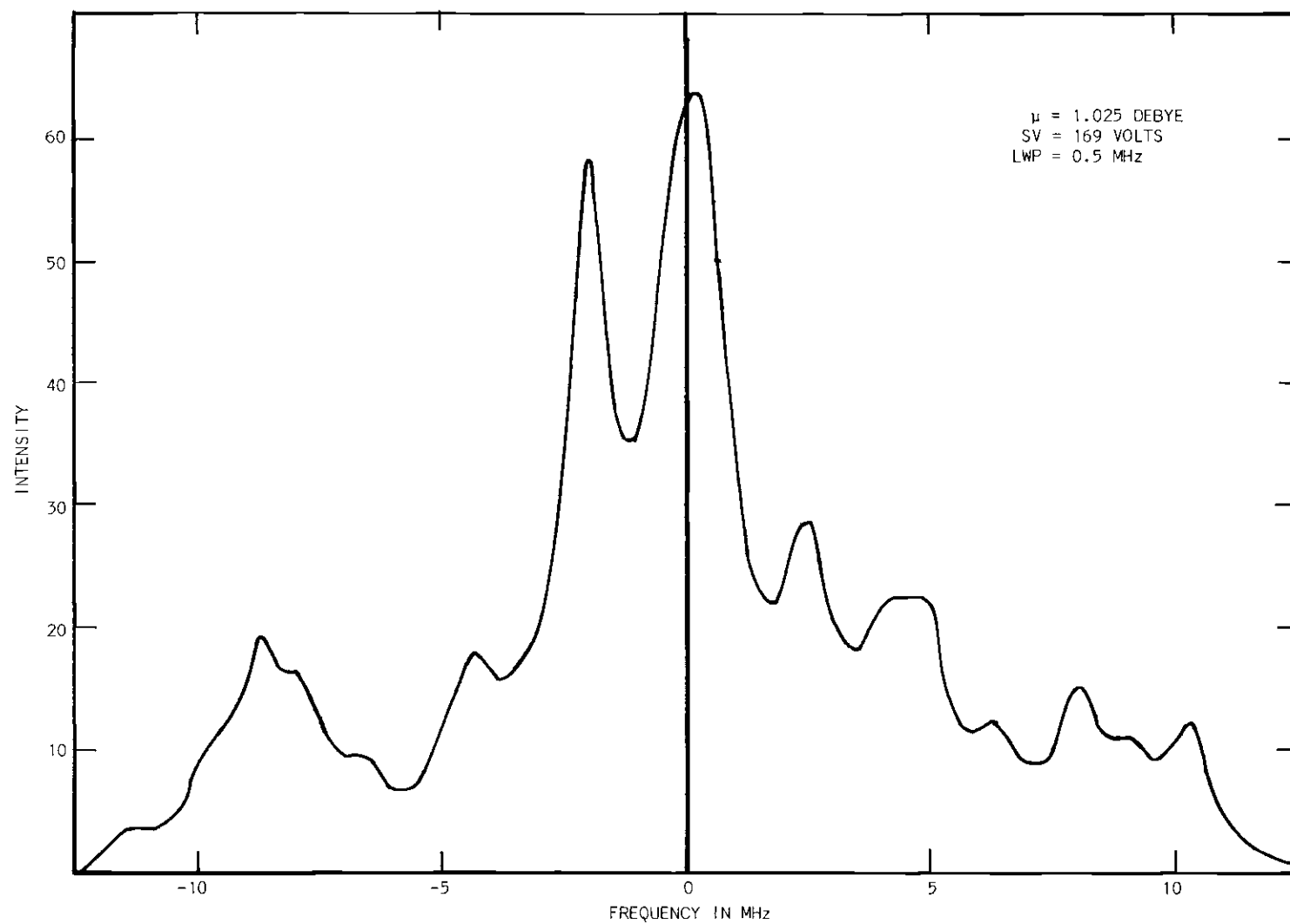


Figure 18. Calculated Pressure Broadened Spectrum for the
 $J = 2 - 3$ Transition of CHCl_3 .

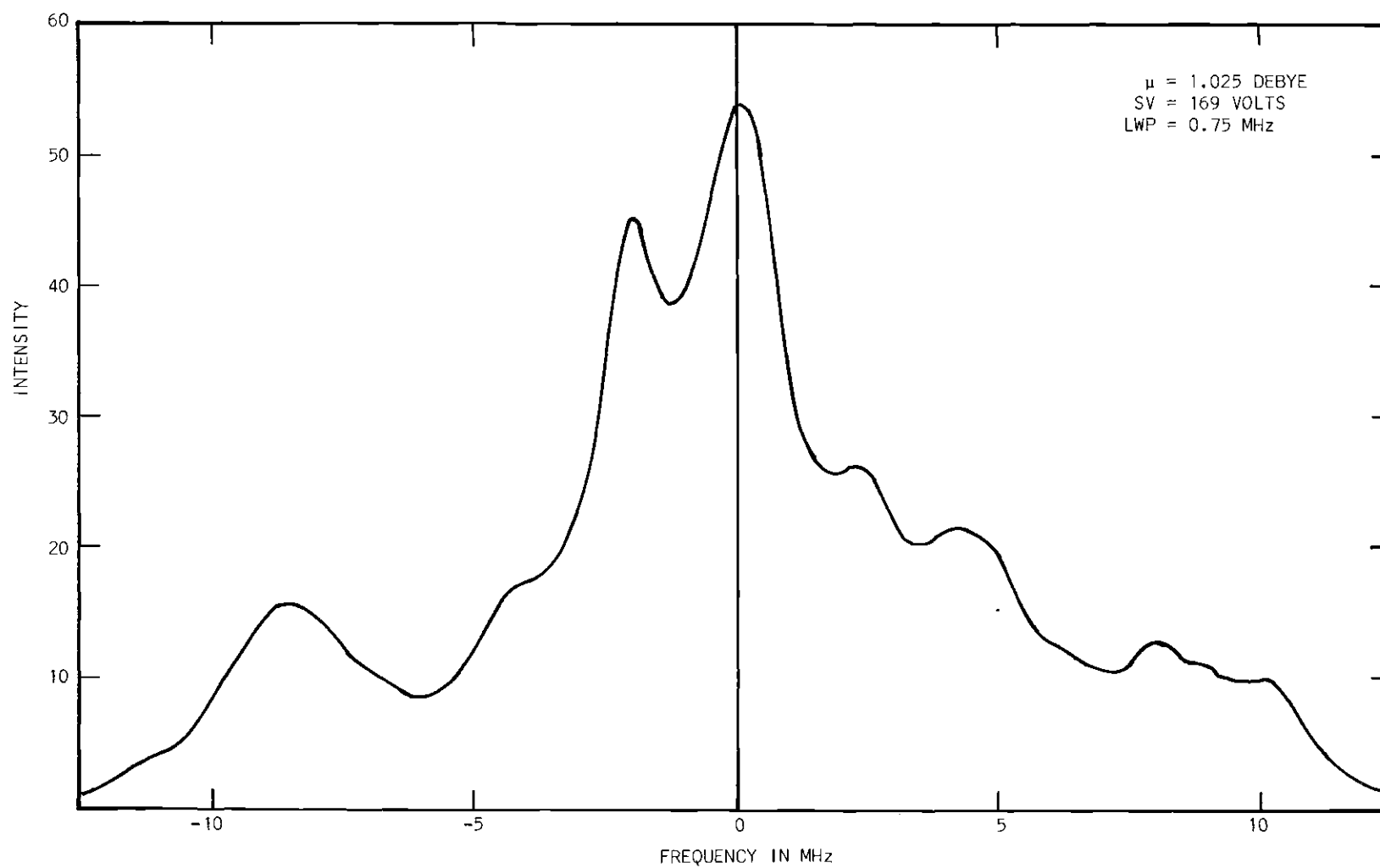


Figure 19. Calculated Pressure Broadened Spectrum for the $J = 2 - 3$ Transition of CHCl_3 .

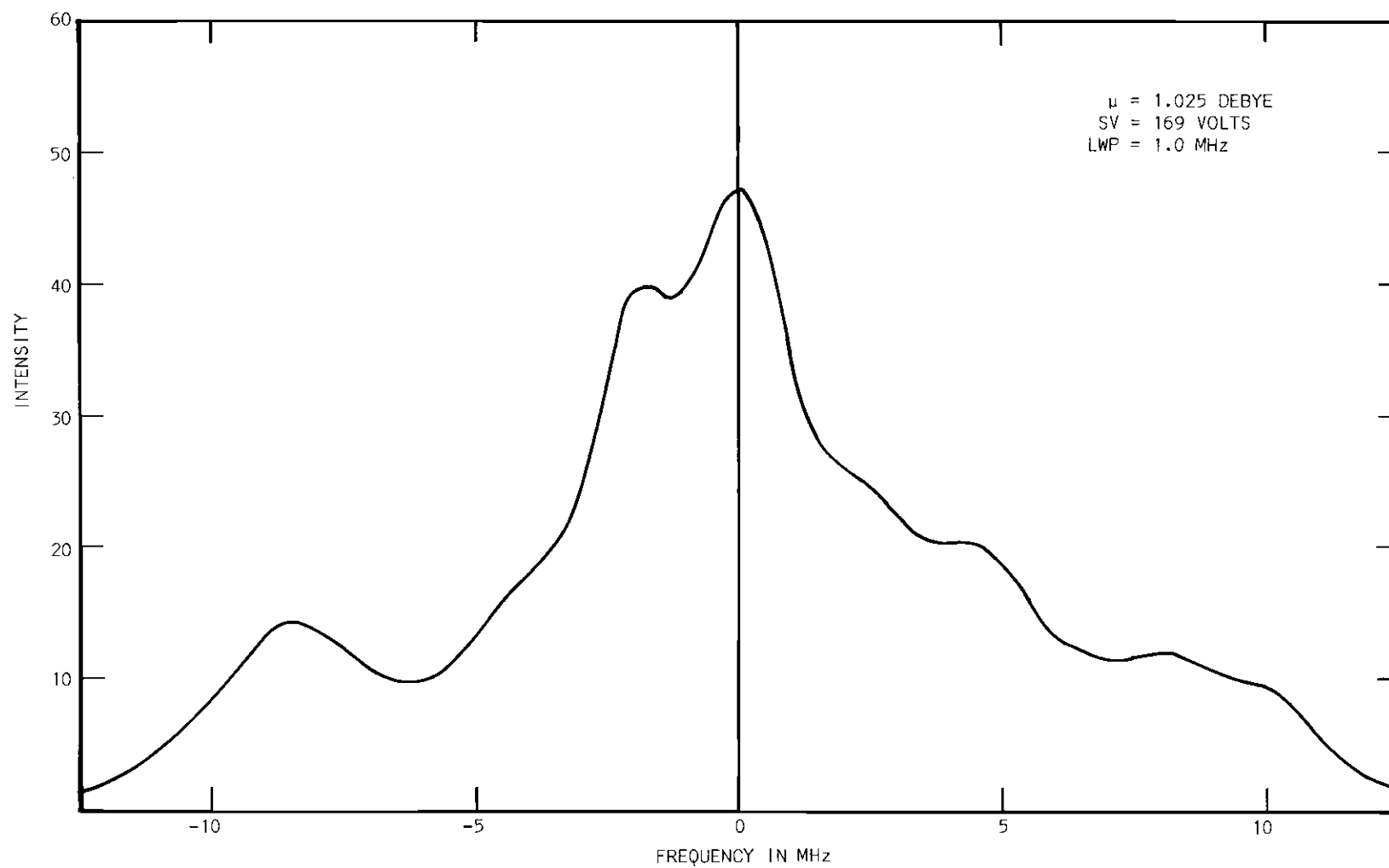


Figure 20. Calculated Pressure Broadened Spectrum for the $J = 2 - 3$ Transition of CHCl_3 .

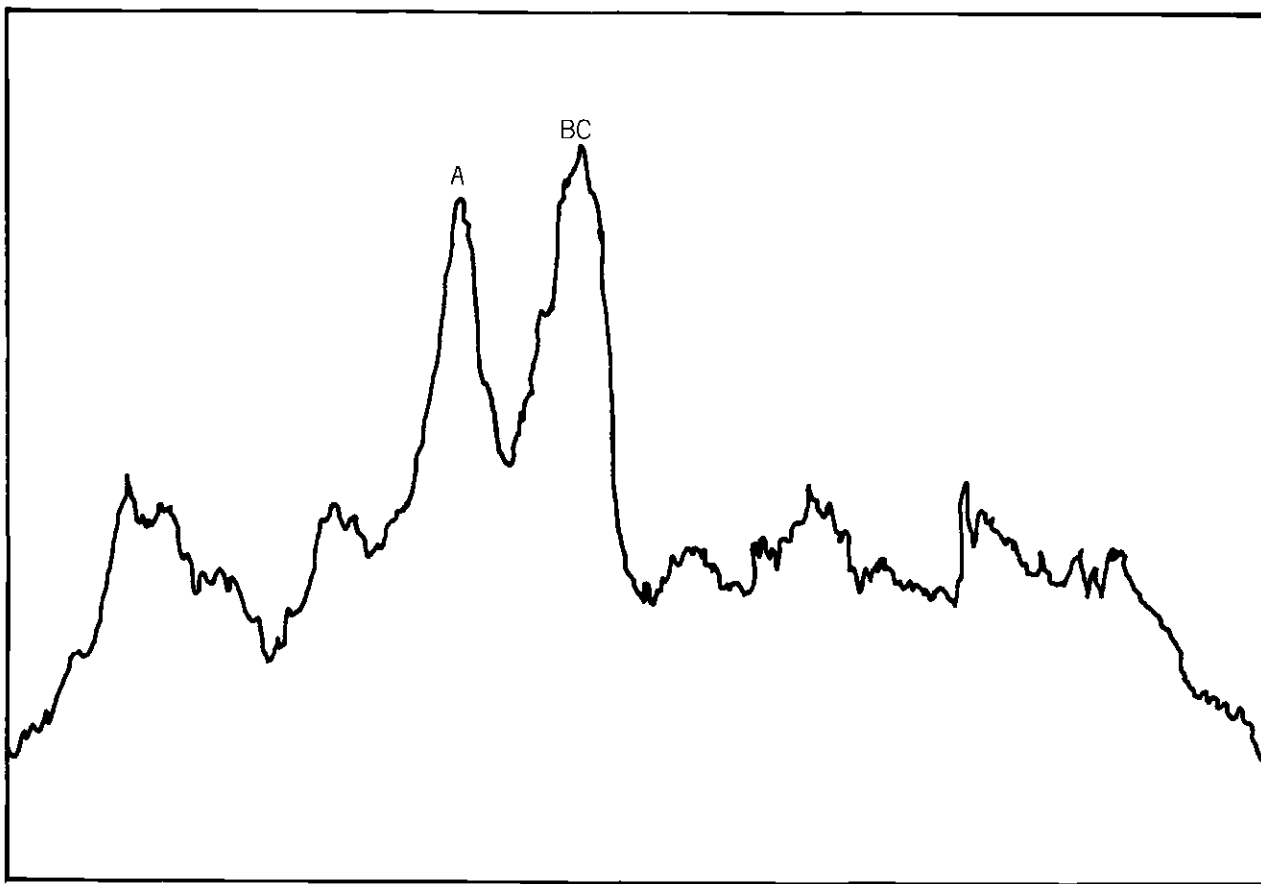


Figure 21. Measured Spectrum of CHCl_3 .

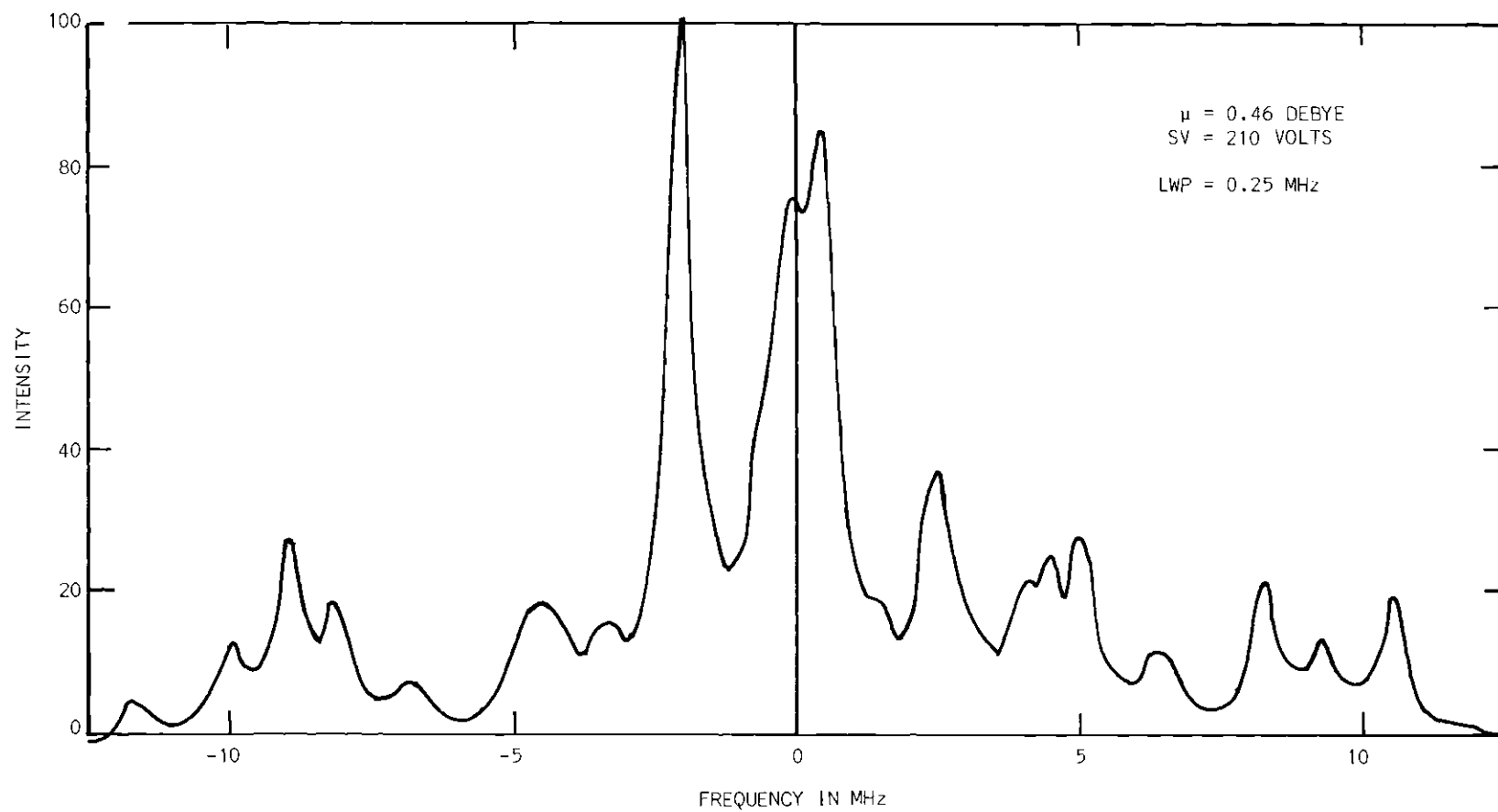


Figure 22. Calculated Pressure Broadened Spectrum for the $J = 2 - 3$ Transition of CFCl_3 .

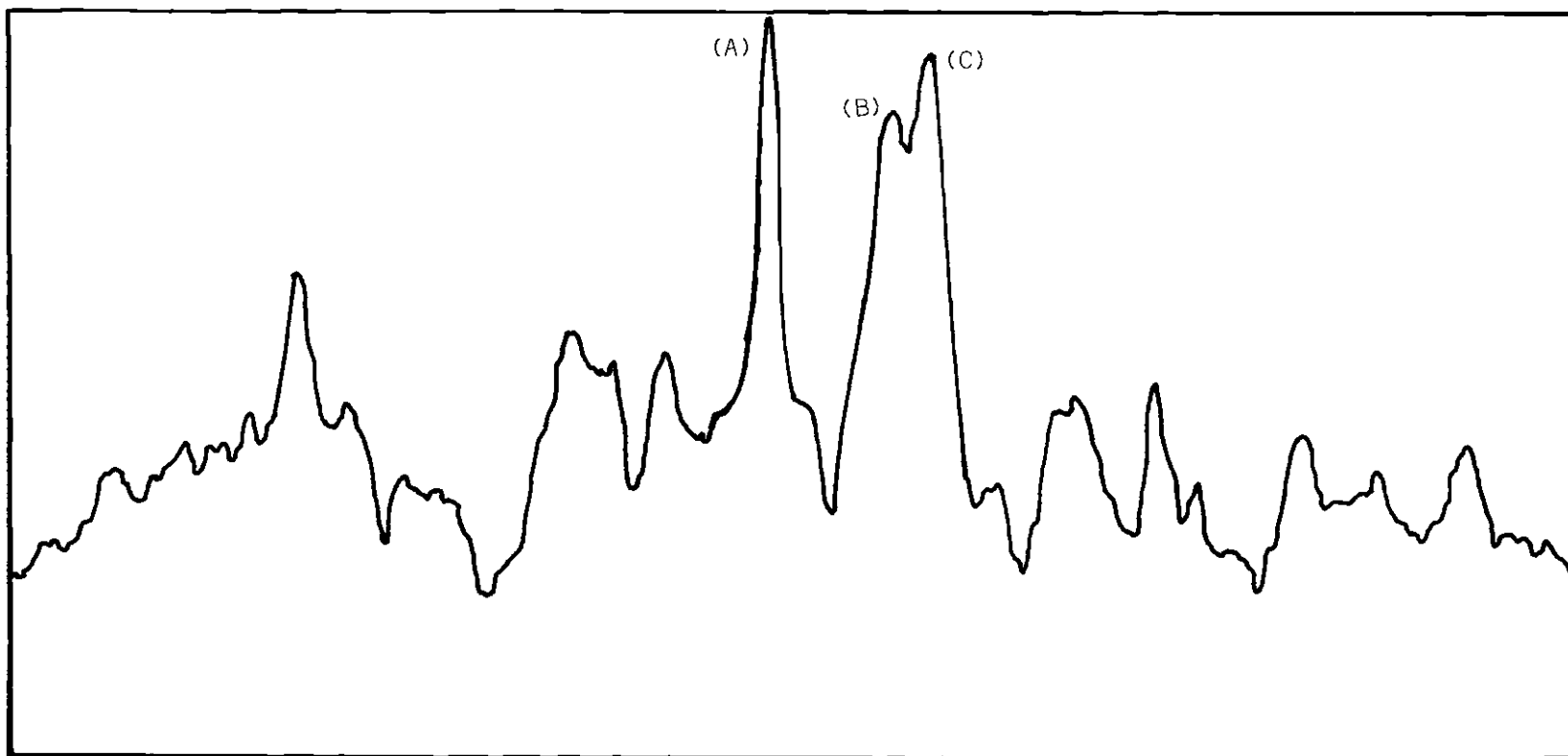


Figure 23. Measured Spectrum of CFCl₃.

For this molecule it was possible to make measurements at a low enough pressure that lines B and C were resolved and Line A was more intense than B or C.

Using the beat note technique, the frequencies of A, B, and C were measured for both CHCl_3 and CFCl_3 . The results of these measurements are compared with A. A. Wolf's measurements and with predicted values in Table 2.

Table 2. Frequencies of the High Intensity Lines in
the $J = 2 - 3$ Transitions of CHCl_3 and CFCl_3 .

Molecule	Source	Operating Conditions	A	B	C
CHCl_3	A. A. Wolf ⁽³¹⁾	178°C, 5 Hg, 300v/cm	19810.21 +0.04MHz	19812.24 +0.08MHz	19812.66 +0.08MHz
	Present work	-78°C, 15 Hg, 341v/cm	19810.25 +0.07	19812.45 +0.07	19812.45 +0.07
	Computed	See Figure 18	19810.25 +0.20	19812.50 +0.2	19812.50 +0.2
CFCl_3	A. A. Wolf ⁽³²⁾	-78°C, 15 Hg, 200v/cm	14792.82 +0.03	14794.72 +0.05	14795.44 +0.05
	Present work	-78°C, 15 Hg, 457v/cm	14792.75 +0.07	14794.78 +0.07	14795.41 +0.07
	Computed	See Figure 22	14792.75 +0.2	14794.75 +0.2	14795.25 +0.2

Since the purpose of this table is to compare calculated and observed quadrupole splitting the rotational constant has been adjusted to make the calculated frequency of line A agree with the measured frequency. The calculated frequencies of lines B and C then fall within the experimental errors of the measured B and C.

CHAPTER V

CONCLUSIONS AND RECOMMENDATIONS

Dipole moment measurements for CHCl_3 and CFCl_3 were made using both the Double Phase-Lock Stabilization technique and the Beat note technique. Using weighted averages of the results of these measurements, the dipole moment of CHCl_3 was found to be 1.04 ± 0.02 debye and the dipole moment of CFCl_3 was found to be 0.46 ± 0.02 debye. The weighting factors were inversely proportional to the square of the size of the 90 per-cent confidence interval.

Inherently, the double phase-lock stabilization technique (method 1) should be more accurate than the beat note technique (method 2), and it is therefore recommended that attempts to make measurements using this technique not be abandoned. There are several possible factors contributing to the erratic measurements that this researcher obtained when using method 1. The Stark square-wave generator used with method 1 did not produce as good a square-wave pattern as the new solid state square-wave generator used with method 2. Also, different klystrons had to be used in the two measurements, and there is reason to believe that a more stable klystron was used with method 2 than with method 1.

Calculated pressure broadened spectra according to equation III-25 compare well with measured spectra when proper values for the product, bp , are used. Although the comparison is not perfect; nevertheless, the similarity of

the calculated and measured spectra lead one to have confidence in equations III-17, 22, and 25. From Table 2 values for the line width parameter, b , can be estimated for CHCl_3 and CFCl_3 as 0.028 ± 0.014 MHz/mmHg and 0.014 ± 0.007 MHz/mmHg, respectively.

The fact that the line width parameter for CHCl_3 is larger than the line width parameter for CFCl_3 is consistent with the result stated by Townes and Schawlow (33) that the line width parameter is proportional to the square of the matrix element of the dipole moment operator between initial and final states.

The agreement between the calculated and measured spectra illustrated by the figures and the closeness of the measured and calculated frequencies for lines A, B, and C in Table 2 confirm the theory to the degree of accuracy of the measurements.

APPENDIX A
DETERMINING THE EXACT FREQUENCY OF THE SOURCE KLYSTRON
-AN EXAMPLE-

DETERMINING THE EXACT FREQUENCY OF THE SOURCE KLYSTRON

-AN EXAMPLE-

Suppose the following conditions hold:

1. The reference klystron is locked-in at 9.830 GHz.
2. The transfer oscillator's output is at 0.133 GHz.
3. A wavemeter reading of the source klystron's frequency is 19.82 GHz.

One can infer the exact frequency of the source klystron by following the reasoning discussed below.

The second harmonic of the reference klystron's frequency is given by

$$\text{2nd Harmonic (ref. klystron)} = 2 \times 9.830 \text{ GHz} = 19.660 \text{ GHz.} \quad (\text{A-1})$$

The beat notes resulting from mixing this second harmonic with all the harmonics of the transfer oscillator's output are

$$\text{Beatnotes} = 19.660 \pm n (0.133) = \begin{cases} 19.394 \\ 19.527 \\ 19.660 \\ 19.793 \\ 19.926 \\ \vdots \end{cases} \text{ GHz} \quad (\text{A-2})$$

where n is any positive integer.

Since the source klystron is stabilized by a double phase-lock stabilization technique, the possible frequencies at which the source klystron can be locked are plus or minus 30 MHz from the frequencies given by equation A-2:

Possible frequencies For Source Klystron

$$= 19.660 \pm n (0.133) \pm .030 = \left\{ \begin{array}{l} 19.364 \\ 19.424 \\ 19.497 \\ 19.567 \\ 19.630 \\ 19.690 \\ 19.763 \\ 19.823 \\ 19.896 \\ 19.956 \end{array} \right. \text{ gHz.}$$

The wavemeter reading of 19.82 gHz enables one to conclude that the source frequency is in fact 19.823 gHz.

APPENDIX B
ENUMERATION OF BASIS FUNCTIONS

ENUMERATION OF BASIS FUNCTIONS

The first set of basis functions considered in this thesis had the form:

$$U(vJKM_J, m_1, m_2, m_3) = \Psi_{el} \text{ (ground state)} \quad (B-1)$$

$$\cdot \Psi_{vib}(v = 0 \text{ or } 1) \Psi_{rot}(J, K, M_J) \prod_{i=1}^3 u_i(3/2 m_i).$$

For $J = 2$ there are 3200 distinct functions of this form. This fact becomes more apparent when one realizes that v can take on two values (0 or 1), that M_J and K each can take on 5 values $(-2, -1, 0, 1, 2)$, and that each of the three m_i can take on four values $(-3/2, -1/2, 1/2, 3/2)$. Thus there are $2 \times 5^2 \times 4^3 = 3200$ distinct basis functions for the $J = 2$ level.

For the $J = 3$ level the only difference is that M_J and K each can take on 7 values $(-3, -2, -1, 0, 1, 2, 3)$. However, basis functions for which K is ± 3 are not used since the selection rule on K for a transition from J to $J + 1$ is $\Delta K = 0$ and the $J = 2$ level has no basis functions corresponding to $K = 3$. Thus, it is only necessary to consider $2 \times 7 \times 5 \times 4^3 = 4480$ distinct basis functions for the $J = 3$ levels.

The space spanned by the basis functions of the form given in equation B-1 is the same space that is spanned by the basis functions which are ultimately used in the calculation of the Hamiltonian matrix. Yet, one can note that the computer program PBRTAPE does not compute any $K = 0$ levels or transitions.

There are two reasons why those levels and transitions are not computed:

1. The Stark splittings for the $K = 0$ levels are small at the low values of electric field strength used and thus the $K = 0$ spectra in the Stark-field-on case and in the Stark-field-off case are essentially the same and the difference spectrum which is recorded is zero, and 2. PBRTAPE already takes one and one half hours to run with the transitions it does compute. The effect of ignoring the $K = 0$ spectrum is that only 2560 functions are needed to span the $J = 2$ level and only 3584 functions to span the $J = 3$ level.

APPENDIX C
TABLES
NEEDED FOR MATRIX ELEMENT CALCULATIONS

Table 3. The Permutation Group on Three Objects

REPRESENTATION	GROUP ELEMENTS					
	(0)	(123)	(132)	(23)	(31)	(12)
$A^{(1)}$	1	1	1	1	1	1
$A^{(2)}$	1	1	1	-1	-1	-1
E	$\begin{pmatrix} 1 & 0 \\ 0 & 1 \end{pmatrix}$	$\begin{pmatrix} -\frac{1}{2} & -\frac{\sqrt{3}}{2} \\ \frac{\sqrt{3}}{2} & -\frac{1}{2} \end{pmatrix}$	$\begin{pmatrix} -\frac{1}{2} & \frac{\sqrt{3}}{2} \\ -\frac{\sqrt{3}}{2} & -\frac{1}{2} \end{pmatrix}$	$\begin{pmatrix} -1 & 0 \\ 0 & 1 \end{pmatrix}$	$\begin{pmatrix} \frac{1}{2} & \frac{\sqrt{3}}{2} \\ \frac{\sqrt{3}}{2} & -\frac{1}{2} \end{pmatrix}$	$\begin{pmatrix} \frac{1}{2} & -\frac{\sqrt{3}}{2} \\ -\frac{\sqrt{3}}{2} & -\frac{1}{2} \end{pmatrix}$

Table 4. The Genealogical Coefficients

I L	A_1			A_2	E_1				E_2			
	$\frac{3}{2}$	$\frac{5}{2}$	$\frac{9}{2}$	$\frac{3}{2}$	$\frac{1}{2}$	$\frac{3}{2}$	$\frac{5}{2}$	$\frac{7}{2}$	$\frac{1}{2}$	$\frac{3}{2}$	$\frac{5}{2}$	$\frac{7}{2}$
0				$-\sqrt{\frac{1}{6}}$		$+\sqrt{\frac{5}{6}}$						
1	$-\sqrt{\frac{7}{10}}$	$\sqrt{\frac{8}{15}}$							± 1	$-\sqrt{\frac{3}{10}}$	$-\sqrt{\frac{7}{15}}$	
2				$\sqrt{\frac{5}{6}}$	± 1	$-\sqrt{\frac{1}{6}}$	± 1	± 1				
3	$\sqrt{\frac{3}{10}}$	$\sqrt{\frac{7}{15}}$	1							$-\sqrt{\frac{7}{10}}$	$-\sqrt{\frac{8}{15}}$	∓ 1

Table 5. The Reduction Coefficients

$C(A^{(1)}, \frac{3}{2}, \frac{3}{2}) = \frac{3}{5}$	$C(E_1, \frac{5}{2}, \frac{5}{2}) = \frac{3\sqrt{21}}{35}$
$C(A^{(1)}, \frac{3}{2}, \frac{5}{2}) = \frac{4\sqrt{6}}{5}$	$C(E_1, \frac{5}{2}, \frac{7}{2}) = \frac{36\sqrt{7}}{35}$
$C(A^{(1)}, \frac{5}{2}, \frac{5}{2}) = \frac{-\sqrt{21}}{10}$	$C(E_1, \frac{7}{2}, \frac{7}{2}) = \frac{3\sqrt{42}}{7}$
$C(A^{(1)}, \frac{5}{2}, \frac{9}{2}) = \frac{-3}{2}$	$C(E_2, \frac{1}{2}, \frac{3}{2}) = \frac{-3\sqrt{3}}{5}$
$C(A^{(1)}, \frac{9}{2}, \frac{9}{2}) = \frac{-\sqrt{33}}{2}$	$C(E_2, \frac{3}{2}, \frac{3}{2}) = \frac{3}{5}$
$C(A^{(2)}, \frac{3}{2}, \frac{3}{2}) = -1$	$C(E_2, \frac{1}{2}, \frac{5}{2}) = \frac{\sqrt{42}}{10}$
$C(E_1, \frac{1}{2}, \frac{3}{2}) = \frac{-\sqrt{3}}{5}$	$C(E_2, \frac{3}{2}, \frac{5}{2}) = \frac{-9}{5}$
$C(E_1, \frac{3}{2}, \frac{3}{2}) = \frac{11}{5}$	$C(E_2, \frac{3}{2}, \frac{7}{2}) = \frac{6\sqrt{3}}{5}$
$C(E_1, \frac{1}{2}, \frac{5}{2}) = \frac{-3\sqrt{42}}{10}$	$C(E_2, \frac{5}{2}, \frac{5}{2}) = \frac{-\sqrt{21}}{35}$
$C(E_1, \frac{3}{2}, \frac{5}{2}) = \frac{-3}{5}$	$C(E_2, \frac{5}{2}, \frac{7}{2}) = \frac{-12\sqrt{7}}{35}$
$C(E_1, \frac{3}{2}, \frac{7}{2}) = \frac{2\sqrt{3}}{5}$	$C(E_2, \frac{7}{2}, \frac{7}{2}) = \frac{-\sqrt{42}}{7}$

APPENDIX D
PBR TAPE
COMPUTER PROGRAM

REGIN	00000100
% QUADRUPOLE HYPERFINE STRUCTURE AND STARK EFFECT FOR SYMMETRIC-TOP	00000200
% MOLECULES WITH THREE IDENTICAL QUADROPOLAR NUCLEI	00000300
%	00000400
% CALCULATES J=2 TO J=3 SPECTRUM WITH AND WITHOUT STARK FIELD,	00000500
% PRESSURE BROADENS AND TAKES DIFFERENCE OF RESULTANT SPECTRA	00000600
%	00000700
% INPUT DATA CONSISTS OF CL-X-CL BOND ANGLE IN RADIANS, THE	00000800
% QUADRUPOLE COUPLING CONSTANT EQQ IN MC/SEC, THE DIPOLE MOMENT IN	00000900
% DEBYE, THE STARK FIELD IN MC/SEC-DEBYE (I.E., $[V/D] \times .50348$), AND	00001000
% THE LINE WIDTH PARAMETER IN MHZ. THE LINE WIDTH PARAMETER IS	00001100
% THE HALF-WIDTH OF A SINGLE LINE AT HALF-MAXIMUM IN MHZ.	00001200
% THIS PROGRAM REQUIRES THREE DATA CARDS IN THE FOLLOWING ORDER:	00001300
% CARD 1: PUT THE NAME AND CHEMICAL FORMULA OF THE MOLECULE IN	00001400
% THE FIRST 36 SPACES.	00001500
% CARD 2: USING FREE FIELD PUT IN ORDER THE FOLLOWING PARAMETERS:	00001600
% ALPHA1 (THE BOND ANGLE IN RADIANS), EQQ, MU, EFIELD,	00001700
% AND LWP (LINE WIDTH PARAMETER).	00001800
% CARD 3: THIS CONSISTS OF ONE NUMBER AND A COMMA AND TELLS THE	00001900
% COMPUTER WHICH OPTION IS BEING USED. THE OPTIONS ARE AS	00002000
% FOLLOWS:	00002100
% WHAT = 0 MEANS NO CARD OUTPUT.	00002200
% WHAT = 1 MEANS CARD OUTPUT FOR QUADRUPOLE SPECTRUM.	00002300
% WHAT = 2 MEANS CARD OUTPUT FOR STARK SPECTRUM.	00002400
% WHAT = 3 MEANS CARD OUTPUT FOR COMBINED SPECTRUM.	00002500
% WHAT = 4 MEANS AN OUTPUT DATA TAPE IS MADE.	00002600
% A GRAPH OF THE VARIOUS SPECTRA CAN BE MADE BY USING THE OUTPUT	00002700
% CARDS ON THE GRAPHING MACHINE.	00002800
% THE OUTPUT DATA TAPE CONTAINS:	00002900
% NU[P1,PAR1], PEAK[P1,PAR1], NU1[PAR1], PEAK1[PAR1] -	00003000
% I.E. ALL THE QUADRUPOLE PLUS STARK FREQUENCIES AND INTENSITIES	00003100
% AND ALL THE QUADRUPOLE FREQUENCIES AND INTENSITIES.	00003200
% INTEGER PAR,N4,MIN1,EXC,EXP7,P1,PAR1,F1L,MFL ; %	00003300
% INTEGER MF2,I1,I2,R1,C1,MIN4,MIN3,EXP1,D,S,F3,EXP6,F1,F2,V1,V2,	00003400
% N,I,J,K,M,MIN1,N1,N2,N3,MF3,KQ,JQ,K1,JA,JB,K2,L, WHAT;	00003500
% REAL SUMINT1,INT1,LWP,SUMINT,IQ1,FQ1,FQ2,MFQ ; %	00003600
% REAL MEF,TR1,TR2,MF22,F12,F22,I12,SPLIT3,EQQ3,FREQ ; %	00003700

REAL SM1,J1,J2,J3,L1,L2,L3,M1,M2,M3,MU,EFIELD,TE3,TE4 ; %	00003800
REAL ALPHA1,ALP,SUMI,DIPOLE,INT,SPLIT,T2,T3,TRA,TRD,	00003900
SUMX2,SUMY2,SPROD,ITS,FREQ1,FREQ2,SPLIT2,EQQ ; %	00004000
ALPHA A1, A2, A3, A4, A5, A6;	00004100
ARRAY ALP2,BETA2(0:4,0:4),FACT(-10:21) ; %	00004200
ARRAY B1(0:1,1:4,1:6,1:34),B2(0:1,1:4,1:7,1:44),EGY1(0:34),	00004300
B(1:2,1:3,0:1,1:4,1:4,1:9),EGY2(0:44) ; %	00004400
ARRAY NU1,PEAK1(0:1000),E(1:2,1:3,0:1,1:4,1:9) ; %	00004500
ARRAY A,Y,DG(0:45,0:45),PEAK,NU(1:8,1:900),SJSY(0:4,0:6,0:7) ; %	00004600
ARRAY THJS(1:6,1:6,1:7) ; %	00004700
FILE IN CRR(2,10);	00004800
FILE PBRTAPE 2(2,1023, SAVE 180);	00004900
FILE OUT LINE 16(2,15) ; %	00005000
FILE OUT PUNCH 0(2,10);	00005100
LIST SNAFU (TRA,TRD,TRA-TRD),	00005200
INP (N,FOR I = 1 STEP 1 UNTIL N DO	00005300
FOR J = 1 STEP 1 UNTIL N DO A(I,J)) ;	00005400
FORMAT IN LETTERS(6A6);	00005500
FORMAT OUT HEADINT(/"TRANSITIONS J=1,F=",I2,"/2,V=",I2,	00005600
" TO J=2,F=",I2,"/2,V=",I2), %	00005700
SUMINTF("SUM OF INTENSITIES = ", F10.4) , %	00005800
MH("MATRIX FOR J=",I2," MF=",I2,"/2") , %	00005900
IL(/"TRANSITIONS J=3 + J=2 FOR MF=",I2,"/2 FOR K =", I1) , %	00006000
HEAD2("TRANSITIONS FROM J=2,K=2,F=",I2,"/2 TO J=3,K=2"),	00006100
INT2(X4,F10.4,X7,F12.8,X9,F10.4),	00006200
PLOT(X10,2F20.4) , %	00006300
MUE(/" DIPOLE MOMENT =",F5.2," DEBYE,ELECTRIC FIELD = ",F8.3,	00006400
" MC./(SEC-DEBYE), STARK VOLTAGE =",F7.3/) , %	00006500
QUAD1(/" QUADRUPOLE COUPLING CONSTANT EQQ =",F8.3," BOND ANGLE"	00006600
" HAL=X-HAL =",F8.2) , %	00006700
NAME(/"QUADRUPOLE SPECTRA FOR ", 6A6),	00006800
NAMES(/"QUADRUPOLE PLUS STARK INTERACTION SPECTRUM FOR ", 6A6),	00006900
PBSH(" LWP =",F6.3," MHZ."/),	00007000
IH(/X5,"J=",I3," LEVEL",X8,"J=",I3," LEVEL",X9,"SPLITTING",X10,	00007100
"INTENSITY",	00007200
HEAD3(/X5,"J=2 LEVEL",X10,"INTENSITY",X10,"SPLITTING IN MC"/),	00007300
INTENSITY(X4,F10.4,X9,F10.4,X7,F12.6,X7,F12.8,16) , %	00007400

```

PLOT2(/X10,F7.3,3F20.4) , %                                00007500
HEADIN2(/"TRANSITIONS J=",I2,"F=",I2,"/2,V=",I2,          00007600
      " TO J=",I2,"F=",I2,"/2,V=",I2) , %                00007700
JH("TRANSITIONS J=",I3," TO J=",I3,"K=",I3) , %          00007800
PBSH2(/X9,"FREQUENCY",X9,"QUADRUPOLE",X13,"STARK",X11,     00007900
"QUADRUPOLE "/X11,"IN MC",X12,"SPECTRUM",X14,"SPECTRUM",X8, 00008000
"MINUS STARK") , %                                         00008100
EMIT(/X9,"PROCESSOR TIME IS ",F10.6," MIN, IN TIME IS ",  00008200
F10.6," MIN");                                              00008300
FORMAT OUT CHECK ("TRA=",F13.4,X9,"TRD=",F13.4,X9,"DIFF=",F7.4), 00008400
      EIG ("DEGENERATE EIGENVALUE--ORTHONORMALIZED VECTOR IS="),00008500
      DATA ("INPUT MATRIX IS"), %                         00008600
      PBS12(/"PRESSURE BROADENED SPECTRUM FOR J=1 TO J=2 TRANSITIONS"),00008700
      PBS23(/"PRESSURE BROADENED SPECTRUM FOR J=2 TO J=3 TRANSITIONS"),00008800
      DGN ("DIAGONALIZED MATRIX IS") ; %                  00008900
FORMAT DIV7R0("ZERO DENOMINATOR REACHED IN VECTOR CALCULATION" 00009000
"FOR J=",I3,"K=",I3,". VECTOR FOLLOWING IS INVALID") , %   00009100
EXDEG("EXACT DEGENERACY FOR EIGENVALUE",I3,". SCHMIDT PROCESS" 00009200
" BREAKS DOWN") ; %                                        00009300
INTEGER PROCEDURE MIN2(P1,P2,P3,P4) ; %                    00009400
  VALUE P1,P2,P3,P4 ; %                                     00009500
  INTEGER P1,P2,P3,P4 ; %                                   00009600
  BEGIN IF P1<P2 AND P1<P3 AND P1<P4 THEN MIN2<P1 ; %     00009700
        IF P2<P1 AND P2<P3 AND P2<P4 THEN MIN2<P2 ; %     00009800
        IF P3<P1 AND P3<P2 AND P3<P4 THEN MIN2<P3 ; %     00009900
        IF P4<P1 AND P4<P2 AND P4<P3 THEN MIN2<P4 ; END   ;00010000
  REAL PROCEDURE FACA(S) ; % CALCULATES FACTORIAL OF S      00010100
  VALUE S ; INTEGER S ; %                                    00010200
  FACA<IF S<0 THEN 0 ELSE IF S< 2 THEN 1 ELSE FACA(S-1)*S ;00010300
  REAL PROCEDURE DEL(D1,D2,D3) ; %                          00010400
  VALUE D1,D2,D3 ; REAL D1,D2,D3 ; %                       00010500
  DEL = SQRT(FACT(D1+D2+D3)*FACT(D1-D2+D3)*FACT(-D1+D2+D3)/ 00010600
  FACT(D1+D2+D3+1)) ; %                                     00010700
  REAL PROCEDURE SUMK(J1,J2,J3,L1,L2,L3) ;                 00010800
  VALUE J1,J2,J3,L1,L2,L3 ; %                              00010900
  REAL J1,J2,J3,L1,L2,L3 ; %                              00011000
  BEGIN %                                                    00011100

```


SM1←0 ; MIN3←MIN2(J1+J2-J3,J1+L2-L3,L1+J2-L3,L1+L2-J3) ; %	00011200
FOR K←0 STEP 1 UNTIL MIN3 DO BEGIN %	00011300
F3← FACT[K]×FACT[J1+J2-J3-K] %	00011400
×FACT[J1+L2-L3-K]×FACT[L1+J2-L3-K]×FACT[-J1-L1+J3+L3+K] %	00011500
×FACT[-J2-L2+J3+L3+K]×FACT[L1+L2-J3-K] ; %	00011600
IF F3>0 THEN SM1←SM1 + (IF BOOLEAN(K) THEN -1 ELSE 1) %	00011700
×FACT[J1+J2+L1+L2+1-K]/F3 ; END	00011800
SUMK ← SM1 ; %	00011900
END ;	00012000
REAL PROCEDURE SIXJ(J1,J2,J3,L1,L2,L3) ; %	00012100
% CALCULATES WIGNER 6-J COEFFICIENTS	00012200
VALUE J1,J2,J3,L1,L2,L3 ; %	00012300
REAL J1,J2,J3,L1,L2,L3 ; %	00012400
BEGIN %	00012500
EXP1 ← J1+J2+L1+L2 ; %	00012600
IF ABS(J1+J2)≥J3 AND ABS(J1-J2)≤J3 THEN %	00012700
SIXJ ←(IF BOOLEAN(EXP1) THEN -1 ELSE 1) %	00012800
×DEL(J1,J2,J3)×DEL(L1,L2,J3)×DEL(J1,L2,L3)	00012900
× SUMK(J1,J2,J3,L1,L2,L3)× DEL(L1,J2,L3) %	00013000
ELSE SIXJ←0 ; %	00013100
END ; %	00013200
REAL PROCEDURE SUMK2(J1,J2,J3,M1,M2,M3) ; %	00013300
VALUE J1,J2,J3,M1,M2,M3 ; %	00013400
REAL J1,J2,J3,M1,M2,M3 ; %	00013500
BEGIN %	00013600
SM1←0 ; MIN3←MIN2(J1+J2-J3,J1-M1,J2+M2,100) ; %	00013700
FOR K←0 STEP 1 UNTIL MIN3 DO BEGIN %	00013800
F3←(FACT[K]×FACT[J1+J2-J3-K]×FACT[J1-M1-K]×	00013900
FACT[J2+M2-K]×FACT[J3-J2+M1+K]×FACT[J3-J1-M2+K])	00014000
IF F3>0 THEN SM1←SM1 + (IF BOOLEAN(K) THEN -1 ELSE 1)/F3 ; END ;	00014100
SUMK2 ← SM1 ; %	00014200
END ; %	00014300
REAL PROCEDURE THREEJ(J1,J2,J3,M1,M2,M3) ; %	00014400
% CALCULATES WIGNER 3-J COEFFICIENTS	00014500
VALUE J1,J2,J3,M1,M2,M3 ; %	00014600
REAL J1,J2,J3,M1,M2,M3 ; %	00014700
BEGIN %	00014800

EXP1 ← J1-J2-M3 ; %	00014900
IF M1+M2+M3≠0 THEN THREEJ←0 ELSE %	00015000
THREEJ← (IF BOOLEAN(EXP1) THEN -1 ELSE 1) %	00015100
×SQRT(FACT[J1+J2-J3]×FACT[J1-J2+J3] %	00015200
×FACT[-J1+J2+J3]×FACT[J1+M1]×FACT[J1-M1] ×FACT[J2+M2]	00015300
×FACT[J2-M2]×FACT[J3+M3]×FACT[J3-M3]/FACT[J1+J2+J3+1])	00015400
×SUMK2(J1,J2,J3,M1,M2,M3) ; %	00015500
END ; %	00015600
REAL PROCEDURE QDP(J,F1,I1,I2,V1,K) ;	00015700
% CALCULATES QUADRUPOLE INTERACTION MATRIX ELEMENT	00015800
VALUE J,F1,I1,I2,V1,K ; %	00015900
REAL J,F1,I1,I2,V1,K ; %	00016000
BEGIN INTEGER EXP4,EXP5 ; %	00016100
EXP4← 2 + 3/2 +J+F1 ; EXP5← J+V1+3 ; %	00016200
IF K =1 THEN	00016300
QDP← (-1)*EXP4×SIXJ(2,J,J,F1,I2,I1)×SQRT(5)	00016400
×(ALP2[(2×I1+1)/2,(2×I2+1)/2]×SQRT(2×J+1)×(3×K+2-J×(J+1))	00016500
×ALP/SQRT((2×J+3)×(2×J+2)×2×J×(2×J-1))	00016600
+(-1)*EXP5×BETA2[(2×I1+1)/2,(2×I2+1)/2]×SQRT(2×J+1)	00016700
×J×(J+1)×(ALP-1)/(2×SQRT((2×J+3)×(2×J+2)×2×J×(2×J-1)))×EQQ	00016800
ELSE	00016900
QDP← (-1)*EXP4×SIXJ(2,J,J,F1,I2,I1)×SQRT(5)	00017000
×ALP2[(2×I1+1)/2,(2×I2+1)/2]×SQRT(2×J+1)×(3×K+2-J×(J+1))	00017100
×ALP/SQRT((2×J+3)×(2×J+2)×2×J×(2×J-1)) × EQQ	00017200
END	00017300
REAL PROCEDURE STARK(J,JP,I1,F1,F2,MF,K) ; %	00017400
% CALCULATES STARK EFFECT MATRIX ELEMENT	00017500
VALUE J,I1,F1,F2,MF,K,JP ; %	00017600
REAL J,I1,F1,F2,MF,K,JP ; %	00017700
BEGIN EXP6←F1+F2+I1-MF-K ; %	00017800
STARK←(IF BOOLEAN(EXP6) THEN -1 ELSE 1)×THREEJ(F1,I1,F2,-MF,0,MF)	00017900
×SQRT((2×F1+1)×(2×F2+1))×SIXJ(J,F1,I1,F2,JP,1) %	00018000
×SQRT((2×J+1)×(2×JP+1))×THREEJ(JP,J,I1,K,-K,0)×MUEFIELD ; %	00018100
END ; %	00018200
PROCEDURE CLEARA(A) ; %	00018300
ARRAY A[0,0] ; %	00018400
BEGIN %	00018500

```

        FOR I+1 STEP 1 UNTIL 4 DO FOR J+1 STEP 1 UNTIL 4 DO A[I,J]+0;00018600
END CLEARA ; %00018700
INTEGER PROCEDURE MIN(P1,P2) ; %00018800
VALUE P1,P2 ; %00018900
INTEGER P1,P2 ; %00019000
    IF P1 < P2 THEN MIN + P1 ELSE %00019100
    MIN + P2 ; %00019200
PROCEDURE MATRIXPRINT (N,M,A) ; %00019300
VALUE N,M ; %00019400
INTEGER N,M ; %00019500
ARRAY A[0,0] ; %00019600
BEGIN %00019700
    FORMAT OUT FMT ("ROW",I3,X2,"COL",I3,5F20.8 ) ; %00019800
    INTEGER I,J,K ; %00019900
LIST ROW ( I,J, FOR K+ 1 STEP 1 UNTIL MIN1 DO A[I,K] ) ; %00020000
    FOR I + 1 STEP 1 UNTIL N DO ; %00020100
        BEGIN %00020200
            MIN1 + 5 ; %00020300
            J + 1 ; WHILE J ≤ M DO %00020400
                BEGIN %00020500
                    WRITE (LINE,FMT,ROW) ; %00020600
                    I + K ; %00020700
                    MIN1 + MIN(J+4,M) %00020800
                END %00020900
            END %00021000
        END MATRIXPRINT ; %00021100
    PROCEDURE EAGLE(N,A) ; %00021200
% CONTROL PROCEDURE FOR EIGENVALUE AND EIGENVECTOR CALCULATION00021300
    VALUE N ; INTEGER N ; ARRAY A[0,0] ; %00021400
    BEGIN %00021500
        ARRAY REF[0:44,0:44],X,GDOFF[0:44] ; %00021600
        INTEGER ARRAY TD[0:44,0:44] ; %00021700
        FORMAT OUT GDOFF("VECTOR CHECK BY SUM OF PRODUCTS FOR ROW",I2,F12.8,00021800
            I4) ; %00021900
        LIST GDOFF (I,GDOFF[I],K) ; %00022000
        LABEL TOM ; %00022100
% CALL CAST A TAPE PROCEDURE A016 FOR CALCULATING EIGENVALUES AND00022200

```

% EIGENVECTORS	00022300
\$\$ A A016	00000000
	99999999
FOR I ← 2 STEP 1 UNTIL N DO %	00022400
FOR J ← 1 STEP 1 UNTIL I-1 DO A[I,J] ← A[J,I] ; %	00022500
FOR I ← 1 STEP 1 UNTIL N DO FOR J ← 1 STEP 1 UNTIL N DO	00022600
BEGIN %	00022700
REF[I,I] ← A[I,J] ; %	00022800
IF I = J THEN ID[I,J] ← 1 ; %	00022900
IF I ≠ J THEN ID[I,J] ← 0 %	00023000
END ; %	00023100
TRA ← 0.0 ; %	00023200
FOR I ← 1 STEP 1 UNTIL N DO %	00023300
TRA ← TRA + A[I,I] ; %	00023400
% CALCULATE EIGENVALUES AND EIGENVECTORS	00023500
JACOBI(1,N,A,DG) ; %	00023600
TRD ← 0.0 ; %	00023700
FOR I ← 1 STEP 1 UNTIL N DO %	00023800
TRD ← TRD + A[I,I] ; %	00023900
% CHECK INVARIANCE OF TRACE UNDER DIAGONALIZING TRANSFORMATION	00024000
IF ABS(TRA - TRD) > 10 ⁻⁶ THEN %	00024100
WRITE (LINE,CHECK,SNFU) ; %	00024200
% CHECK HOMOGENEITY CONDITION ON EIGENVECTORS	00024300
FOR K ← 1 STEP 1 UNTIL N DO BEGIN %	00024400
FOR I ← 1 STEP 1 UNTIL N DO %	00024500
BEGIN GOOF[I] ← 0.0 ; %	00024600
FOR J ← 1 STEP 1 UNTIL N DO %	00024700
GOOF[I] ← GOOF[I] + (REF[I,J] - A[K,K] × ID[I,J]) × DG[J,K] ; %	00024800
IF GOOF[I] > 10 ⁻⁶ THEN %	00024900
WRITE(LINE,GOOFF,GOOFFO) %	00025000
END ; %	00025100
END ; %	00025200
END EAGLE ; %	00025300
WRITE(LINE[N0]) ; %	00025400
T2 ← TIME(2) ; %	00025500
T3 ← TIME(3) ; %	00025600
READ (CRR, LETTERS, A1, A2, A3, A4, A5, A6);	00025700

```

      READ (CRR, /, ALPHA1, EQQ, MU, EFIELD, LWP);
      READ (CRR, /, WHAT);
      CLOSE(CRR, RELEASE);
      BEGIN REAL DUMMY1 ; %
% BUILD FACTORIAL TABLE
      FOR I=-10 STEP 1 UNTIL 20 DO FACT[I]=FACA(I) ; %
% BUILD TABLE OF REDUCTION COEFFICIENTS C(+) AND C(-)
      ALP2[4,4]=SQRT(42)/7 ; ALP2[3,4]=12*SQRT(7)/35 ; %
      ALP2[3,3]=SQRT(21)/35 ; ALP2[2,4]=4*SQRT(3)/5 ; %
      ALP2[2,3]=-6/5 ; ALP2[2,2]=7/5 ; ALP2[1,3]=-SQRT(42)/10 ; %
      ALP2[1,2]=-2*SQRT(3)/5 ; BETA2[4,4]=-2*SQRT(42)/7 ; %
      BETA2[3,4]=-2*ALP2[3,4] ; BETA2[3,3]=-2*ALP2[3,3] ; %
      BETA2[2,4]=2*SQRT(3)/5 ; BETA2[2,3]=-3/5 ; BETA2[2,2]=-4/5 ;
      BETA2[1,3]=2*SQRT(42)/10 ; BETA2[1,2]=-SQRT(3)/5 ; %
      FOR I=1 STEP 1 UNTIL 4 DO FOR L=1 STEP 1 UNTIL I DO %
      BEGIN ALP2[I,L]=ALP2[L,I] ; BETA2[I,L]=BETA2[L,I] END ; %
      ALP = COS(ALPHA1);
% BUILD TABLE OF WIGNER 6-J SYMBOLS
      FOR IQ1=1 STEP 1 UNTIL 4 DO FOR FQ1=1 STEP 1 UNTIL 6 DO %
      FOR FQ2=1 STEP 1 UNTIL 7 DO IF ABS(FQ1-FQ2) ≤ 1 THEN %
      SJSY[IQ1,FQ1,FQ2]=SIXJ(2,(2*FQ1-1)/2,(2*IQ1-1)/2,(2*FQ2-1)/2,3,1) ;
% BUILD TABLE OF WIGNER 3-J SYMBOLS
      FOR MFQ=1 STEP 1 UNTIL 6 DO FOR FQ1=MFQ STEP 1 UNTIL 6 DO %
      FOR FQ2=MFQ STEP 1 UNTIL 7 DO IF ABS(FQ1-FQ2) ≤ 1 THEN %
      THJS[MFQ,FQ1,FQ2]=THREEJ((2*FQ1-1)/2,1,(2*FQ2-1)/2,
      -(2*MFQ-1)/2,0,(2*MFQ-1)/2) ; %
      WRITE(LINE,NAMES,A1,A2,A3,A4,A5,A6); %
      WRITE(LINE,QUAD1,EQQ,ALPHA1*57.2958) ; %
      PAR = 0; SUMINT = 0; %
% CALCULATE MATRICES FOR STARK PLUS QUADRUPOLE INTERACTION
      FOR KQ=1,2 DO
      BEGIN FOR MF2=11 STEP -2 UNTIL 1 DO BEGIN
      FOR K1=1 STEP 1 UNTIL 34 DO EGY1[K1]=0 ; %
      FOR K1=1 STEP 1 UNTIL 44 DO EGY2[K1]=0 ; %
      FOR I1=1,2,3,4 DO FOR F1=1,2,3,4,5,6 DO FOR V1=0,1 DO FOR K1=1 %
      STEP 1 UNTIL 34 DO R1[V1,I1,F1,K1]=0 ; %
      FOR I1=1,2,3,4 DO FOR F1=1,2,3,4,5,6 DO FOR V1=0,1 DO FOR K1=1 %

```

```

STEP 1 UNTIL 44 DO B2[V1,I1,F1,K1]←0 ; % 00029500
BEGIN FOR JQ←2,3 DO % 00029600
  BEGIN R1←C1+N←0 ; % 00029700
  FOR F1←2×JQ+7 STEP -2 UNTIL ABS(MF2) DO % 00029800
    BEGIN MIN4←MIN(7,F1+2×JQ) ; FOR I1←MIN4 STEP -2 WHILE % 00029900
      I1≥ABS(F1-2×JQ) DO FOR V1←0,1 DO BEGIN C1←R1 ; R1←R1+1 ; % 00030000
        FOR F2←F1 STEP -2 UNTIL ABS(MF2) DO BEGIN MIN3←MIN(7,F2+2×JQ) ; 00030100
          FOR I2← IF F2=F1 THEN I1 ELSE MIN3 STEP -2 WHILE % 00030200
            I2≥ABS(F2-2×JQ) DO FOR V2← IF F2=F1 AND I2=I1 THEN V1 ELSE 0 STEP 00030300
              1 UNTIL 1 DO % 00030400
                BEGIN C1←C1+1 ; N←C1 ; % 00030500
                IF F1-F2≤2 AND I1=I2 AND V1≠V2 THEN % 00030600
                  A[R1,C1]←STARK(JQ,JQ,I1/2,F1/2,F2/2,MF2/2,KQ) ELSE % 00030700
                  IF F1=F2 AND V1=V2 THEN A[R1,C1]←QDP(JQ,F1/2,I1/2,I2/2,V1,KQ) 00030800
                  ELSE A[R1,C1]←0 ; END END END END ; % 00030900
                EAGLE(N,A) ; % 00031000
% ASSIGN QUANTUM NUMBERS TO ENERGY EIGENVALUES AND 00031100
% EIGENVECTOR COMPONENTS 00031200
  FOR K1←1 STEP 1 UNTIL N DO % 00031300
    BEGIN I←0 ; FOR F1←2×JQ+7 STEP -2 UNTIL ABS(MF2) DO % 00031400
      BEGIN MIN4←MIN(7,F1+2×JQ) ; FOR I1←MIN4 STEP -2 WHILE % 00031500
        I1≥ABS(F1-2×JQ) DO FOR V1←0,1 DO BEGIN I←I+1 ; % 00031600
          IF JQ=2 THEN BEGIN B1[V1,(I1+1)/2,(F1+1)/2,K1]←DG[I,K1] ; % 00031700
            EGY1[K1]←A[K1,K1] ; N1←N END ; % 00031800
          IF JQ=3 THEN BEGIN B2[V1,(I1+1)/2,(F1+1)/2,K1]←DG[I,K1] ; % 00031900
            EGY2[K1]←A[K1,K1] ; N2←N END ; % 00032000
        END END ; % 00032100
      END END ; % 00032200
% BEGINNING OF INTENSITY CALCULATION 00032300
  WRITE(LINE,IL,MF2,KQ) ; WRITE(LINE,IH,2,3) ; % 00032400
  MFL←ABS((MF2+1)/2) ; % 00032500
  MF22←MF2/2 ; % 00032600
  JA←1 ; JB←2 ; FOR K1←1 STEP 1 UNTIL N1 DO FOR K2←1 STEP 1 UNTIL N2 DO 00032700
    BEGIN SUMI←0 ; FOR F2←7 STEP -1 UNTIL MFL DO % 00032800
      BEGIN ITS←MIN(4,F2+1) ; % 00032900
      F1L←(IF F2=MFL THEN F2 ELSE F2-1) ; % 00033000
      FOR F1←ITS STEP -1 UNTIL F1L DO % 00033100

```

BEGIN MIN4+MIN2(4,F1+1,F2+2,20) ; %	00033200
F12+ (2×F1-1)/2 ; F22+(2×F2-1)/2 ; %	00033300
IF KQ=1 THEN MEF←4×SQRT((2×F1×F2)/3)×THJS[(MF2+1)/2,F1,F2] ELSE	00033400
MEF←-2×SQRT((5×F1×F2)/3)×THJS[(MF2+1)/2,F1,F2] ;	00033500
FOR I1←MIN4 STEP -1	00033600
WHILE I1≥1 AND I1≥F1-1 AND I1≥F2-2 DO %	00033700
BEGIN I12+(2×I1-1)/2 ; %	00033800
FOR V1←0,1 DO BEGIN V2←IF V1=0 THEN 1 ELSE 0 ; TB1←B1[V1,I1,F1,K1] ;	00033900
TB2←B2[V2,I1,F2,K2] ; IF TB1≠0 AND TB2≠0 THEN %	00034000
BEGIN IF KQ=1 THEN EXP6←F1+F2+I12-MF22 ELSE	00034100
EXP6←F1+F2+I12-MF22+1 ;	00034200
SUMI←SUMI+TB1×TB2×(IF BOOLEAN(EXP6) THEN -1 ELSE 1) %	00034300
×SJSY[I1,F1,F2]×MEF ; %	00034400
END END END END END ; %	00034500
INT←SUMI×2 ; SPLIT← EGY2[K2]-EGY1[K1] ; PAR←PAR+1 ; %	00034600
SUMINT←SUMINT+INT ; IF PAR ≤ 900 THEN %	00034700
BEGIN PEAK[1,PAR]←INT ; NU[1,PAR]←SPLIT END ELSE IF PAR≤1800 THEN	00034800
BEGIN PEAK[2,PAR-900]←INT ; NU[2,PAR-900]←SPLIT END ELSE	00034900
IF PAR ≤ 2700 THEN %	00035000
BEGIN PEAK[3,PAR-1800]←INT ; NU[3,PAR-1800]←SPLIT END ELSE %	00035100
IF PAR ≤ 2700 THEN %	00035200
BEGIN PEAK[3,PAR-1800]←INT ; NU[3,PAR-1800]←SPLIT END ELSE %	00035300
IF PAR ≤ 3600 THEN %	00035400
BEGIN PEAK[4,PAR-2700]←INT ; NU[4,PAR-2700]←SPLIT END ELSE %	00035500
IF PAR ≤ 4500 THEN %	00035600
BEGIN PEAK[5,PAR-3600]←INT ; NU[5,PAR-3600]←SPLIT END ELSE %	00035700
IF PAR ≤ 5400 THEN %	00035800
BEGIN PEAK[6,PAR-4500]←INT ; NU[6,PAR-4500]←SPLIT END ELSE %	00035900
IF PAR ≤ 6300 THEN %	00036000
BEGIN PEAK[7,PAR-5400]←INT ; NU[7,PAR-5400]←SPLIT END ELSE %	00036100
BEGIN PEAK[8,PAR-6300]←INT ; NU[8,PAR-6300]←SPLIT END ; %	00036200
IF INT > 0.01 THEN %	00036300
WRITE(LINE,INTENSITY,EGY1[K1],EGY2[K2],SPLIT,INT,PAR) ; %	00036400
END ; %	00036500
END END END ; %	20036600
WRITE(LINE[DBL]) ; %	00036700
WRITE(LINE,SUMINTF,SUMINT) ; %	00036800

```

WRITE(LINE,EMIT,(TIME(2)-T2)/3600,(TIME(3)-T3)/3600);
BEGIN REAL DUMMY2 ; %
LABEL WORK ; %
N3+1 ; FOR JQ+2,3 DO %
BEGIN N3+ IF N3=2 THEN 1 ELSE 2 ; FOR KQ+1,2,3 DO FOR F1+1 %
STEP 1 UNTIL 9 DO FOR V1+0,1 DO FOR K1+1,2,3,4 DO FOR I1+1,2,3,4
DO %
BEGIN E[N3,KQ,V1,K1,F1]+0 ; B[N3,KQ,V1,K1,I1,F1]+0 %
END ; FOR PAR1+1 STEP 1 UNTIL 1000 DO PEAK1[PAR1]+NU1[PAR1]+0 ;
PAR1+0 ; %
FOR KQ+1 STEP 1 UNTIL JQ DO FOR F1+2×JQ+7 STEP -2 UNTIL 1 DO %
FOR V1+0,1 DO %
BEGIN R1+C1+0 ; CLEAR(A) ; MINI+MIN(7,F1+2×JQ) ; %
% BEGINNING OF CALCULATION FOR QUADRUPOLE INTERACTION ALONE
% CALCULATE MATRIX CORRESPONDING TO CURRENT VALUES OF J,K,F AND V
FOR I1+MINI STEP -2 WHILE I1≥1 AND I1≥F1-2×JQ DO %
BEGIN C1+R1 ; R1+R1+1 ; %
FOR I2+I1 STEP -2 WHILE I2≥1 AND I2≥F1-2×JQ DO %
BEGIN C1+C1+1 ; A[R1,C1]+QDP(JQ,F1/2,I1/2,I2/2,V1,KQ) ; %
END ; %
END ; %
IF JQ=2 AND F1=1 THEN C1+2 ; %
IF JQ=3 AND F1=3 THEN C1+3 ; %
IF JQ=3 AND F1=1 THEN C1+2 ; %
% CALL PROCEDURE TO DIAGONALIZE MATRIX AND CALCULATE EIGENVECTORS
EAGLE(C1,A) ; FOR K1+1 STEP 1 UNTIL C1 DO %
% ASSIGN QUANTUM NUMBERS TO ALL EIGENVALUES AND EIGENVECTOR COMPONENTS
BEGIN E[N3,KQ,V1,K1,(F1+1)/2]+A[K1,K1] ; I1+ MINI +2 ; %
FOR I+1 STEP 1 UNTIL C1 DO %
BEGIN I1+I1-2 ; B[N3,KQ,V1,K1,(I1+1)/2,(F1+1)/2]+DG[I,K1] ;
END ; %
END ; %
END ; %
SUMTNT1+0.0 ; %
IF JQ≠2 THEN FOR KQ+1 STEP 1 UNTIL JQ-1 DO %
BEGIN WRITE(LINE[PAGE]) ; WRITE(LINE,NAME,A1,A2,A3,A4,A5,A6) ; %
WRITE(LINE,QUAD1,EQ0,ALPHA1×57.2958) ; WRITE(LINE,JH,JQ-1,JQ,KQ) ;

```



```

IF KQ =1 THEN WRITE(LINE,IN,JQ-1,JQ) ELSE WRITE(LINE,HEAD3);      00040600
% CALCULATE INTENSITIES FOR ALL TRANSITIONS FROM J TO J+1          00040700
EXC=IF JQ=3 AND KQ=2 THEN 1 ELSE 0 ;00040800
FOR F1=2*(JQ-1)+7 STEP -2 UNTIL 1 DO IF EXC#1 THEN %              00040900
  BEGIN F2=F1 ; %                                                  00041000
WORK:  FOR V1=0,1 DO %                                             00041100
  BEGIN V2=IF V1=0 THEN 1 ELSE 0 ;%                                00041200
    WRITE(LINE,HEADIN2,JQ-1,F1,V1,JQ,F2,V2) ; %                   00041300
    FOR K1=1,2,3,4 DO FOR K2=1,2,3,4 DO %                          00041400
      BEGIN SUMI=0 ; FOR I=4 STEP -1 UNTIL 1 DO %                  00041500
        BEGIN EXP7=1+I+(F2+1)/2 ; N4=IF N3=1 THEN 2 ELSE 1 ; %    00041600
          SUMI=SUMI+B[N4,KQ,V1,K1,I,(F1+1)/2] %                   00041700
          XBIN3,KQ,V2,K2,I,(F2+1)/2)*(IF BOOLEAN(EXP7) THEN -1 % 00041800
          ELSE 1)*SJSY[I,(F1+1)/2,(F2+1)/2] ; %                   00041900
        END ; %                                                    00042000
        INT=(F1+1)*(F2+1)*SUMI*2*(JQ*JQ-KQ*KQ)/(3*JQ) ; %        00042100
        TE3=E[N3,KQ,V2,K2,(F2+1)/2] ; TE4=E[N4,KQ,V1,K1,(F1+1)/2];00042200
        SPLIT=TE3-TE4 ; %                                          00042300
        IF INT#0 THEN BEGIN %                                      00042400
          PAR1=PAR1+1 ; NUI[PAR1]=SPLIT ; PEAK1[PAR1]=INT END ; % 00042500
          SUMINT1=SUMINT1+INT ; %                                   00042600
          IF INT>0.001 THEN %                                       00042700
            WRITE(LINE,INTENSITY,TE4,TE3,SPLIT,INT,PAR1) ; %      00042800
          END ; %                                                  00042900
        END ; %                                                    00043000
        IF F1=F2 THEN BEGIN F2=F1+2 ; GO TO WORK END ; %          00043100
        IF F1#1 AND F2#F1-2 THEN BEGIN F2=F1-2 ; GO TO WORK END ;00043200
        END ELSE BEGIN                                             00043300
          WRITE(LINE,HEAD2,F1) ; FOR K1=1,2,3,4 DO                00043400
        BEGIN INT=0 ; FOR F2=F1+2,F1,F1-2 DO IF F1#1 OR F2#F1-2 THEN 00043500
          BEGIN SUMI=0 ; FOR I=4 STEP -1 UNTIL 1 DO                00043600
            BEGIN EXP7=2+I+(F2+1)/2                                00043700
            INT=INT+ 2*(F1+1)*(F2+1)*(B[N4,KQ,0,K1,I,(F1+1)/2]   00043800
            X(-1)*EXP7*SIXJ(JQ-1,F1/2,(2*I-1)/2,F2/2,JQ,1))*2    00043900
            X(JQ*JQ-KQ*KQ)/(3*JQ);                                00044000
            SPLIT=-E[N4,KQ,0,K1,(F1+1)/2]                          00044100
          END                                                       00044200

```

```

      END
      WRITE(LINE,INT2,"SPLIT,INT,SPLIT");
      PAR1=PAR1+1 ; NU1[PAR1]=SPLIT ; PEAK1[PAR1]=INT ; %
      SUMINT1=SUMINT1+INT ; %
    END
  END ;
  WRITE(LINE,EMIT,(TIME(2)-T2)/3600,(TIME(3)-T3)/3600);
  END END ; %
% LOAD TAPE.
  IF WHAT = 4 THEN BEGIN
    FOR P1=1 STEP 1 UNTIL 8 DO
      BEGIN
        WRITE(PBRTAPE,*,FOR PAR1=1 STEP 1 UNTIL 900 DO NU[P1,PAR1]);
        WRITE(PBRTAPE,*,FOR PAR1=1 STEP 1 UNTIL 900 DO PEAK[P1,PAR1]);
      END;
      WRITE(PBRTAPE,*,FOR PAR1=1 STEP 1 UNTIL 1000 DO NU1[PAR1]);
      WRITE(PBRTAPE,*,FOR PAR1=1 STEP 1 UNTIL 1000 DO PEAK1[PAR1]);
    END;
% PRESSURE BROADEN ALL LINES ACCORDING TO THE VAN VLECK-WEISSKOPF
% RELATION AND ADD TO GET THE RESULTANT SPECTRUM
      WRITE(LINE,SUMINTF,SUMINT1) ; %
      BEGIN ; %
        WRITE(LINE,NAMES,A1,A2,A3,A4,A5,A6); %
        WRITE(LINE,QUAD1,EQQ,ALPHA1*57.2958) ; %
        WRITE(LINE,MUE,MH,EFIELD,EFIELD*0.9554); WRITE(LINE,PBS23) ; %
        WRITE(LINE,PBSH,LWP);
        WRITE(LINE,PBSH2) ; %
        FOR FREQ1= -12.5 STEP 0.25 UNTIL 12.5 DO BEGIN %
          INT=0 ;FOR PAR=1 STEP 1 UNTIL 7000 DO %
            BEGIN IF PAR ≤900 THEN BEGIN P1=1 ; PAR1=PAR END %
              ELSE IF PAR ≤1800 THEN BEGIN P1=2 ; PAR1=PAR-900 END %
              ELSE IF PAR ≤2700 THEN BEGIN P1=3 ; PAR1=PAR-1800 END %
              ELSE IF PAR ≤3600 THEN BEGIN P1=4 ; PAR1=PAR-2700 END %
              ELSE IF PAR ≤4500 THEN BEGIN P1=5 ; PAR1=PAR-3600 END %
              ELSE IF PAR ≤5400 THEN BEGIN P1=6 ; PAR1=PAR-4500 END %
              ELSE IF PAR ≤6300 THEN BEGIN P1=7 ; PAR1=PAR-5400 END %
              ELSE BEGIN P1=8 ; PAR1=PAR-6300 END ; %

```

IF PEAK(P1,PAR1)>0.001 AND ABS(FREQ1-NU[P1,PAR1])<10 THEN %	00048000
INT=INT+(3*PEAK(P1,PAR1)*LWP)/((FREQ1-NU[P1,PAR1])*2*LWP*2);	00048100
END ; %	00048200
INT1=0 ; FOR PAR1=1 STEP 1 UNTIL 1000 DO %	00048300
IF ABS(FREQ1-NU[P1,PAR1])<10 THEN %	00048400
INT1=INT1+(3*PEAK1[PAR1]*LWP)/((FREQ1-NU1[PAR1])*2*LWP*2);	00048500
WRITE(LINE,PLOT2,FREQ1,INT1,INT,INT1-INT) ; %	00048600
IF WHAT = 1 THEN BEGIN	00048700
WRITE(PUNCH,PLOT,50*FREQ1,50*INT1); END;	00048800
IF WHAT = 2 THEN BEGIN	00048900
WRITE(PUNCH,PLOT,50*FREQ1,50*INT); END;	00049000
IF WHAT = 3 THEN BEGIN	00049100
WRITE(PUNCH,PLOT,50*FREQ1,50*(INT1 - INT)); END;	00049200
END;END;END;	00049300
WRITE(LINE,EMIT,(TIME(2)-T2)/3600,(TIME(3)-T3)/3600);	00049400
END;END.	00049500

APPENDIX E
PBRTAPE
THEORY OF OPERATION

PBRTAPE

THEORY OF OPERATION

PBRTAPE can be considered divided into three parts. Part one consists of declarations. This section is the longest because of the many procedures within it. The most important procedures are MIN2(P1, P2, P3, P4); MIN(P1, P2); QDP(J, F1, I1, I2, V1, K); STARK(J, J P, I1, I2, F1, MF, K); and EAGLE(N, A). MIN2 and MIN each have the value of their smallest argument. QDP and STARK each become the value of the matrix element corresponding to their arguments. EAGLE replaces the N-th order, real, symmetric matrix, A, with a diagonal matrix such that the elements $A(I, I)$, $I = 1, 2, \dots, N$ contain the eigenvalues of A arranged in decreasing order of magnitude. The eigenvector associated with the Ith eigenvalue is stored in the I-th column of the matrix DG(I, K). The other procedures are used in the calculation of the procedures discussed above.

Part two begins with the card saying, "WRITE(LINE [NO])," and continues up to the card saying, "PRESSURE BROADEN ALL LINES ACCORDING TO THE VAN VLECK-WEISSKOPF." In this section all relevant data is read into the program, matrix elements are computed, matrices diagonalized, and transition frequencies and intensities are computed for both the quadrupole interaction and the combined Stark and quadrupole interaction. An output tape containing this computed information is made if the appropriate option is exercised.

Part three takes the information computed in part two and computes three pressure broadened spectra: a quadrupole spectrum, a Stark and quadrupole

spectrum, and a difference spectrum.

The Program Segment shown in Figure 24 follows the same logic as part two in PBRTAPE, but is written so that its logic is more transparent. Note the pattern of calculation which this Program Segment follows: 1. A Hamiltonian submatrix is computed, 2. It is diagonalized, 3. The eigenvalues and corresponding eigenfunctions of this submatrix are determined and stored in appropriate arrays, 4. Steps 1-3 are repeated for another Hamiltonian submatrix, and 5. The frequencies and intensities of all transitions between energy levels of the two submatrices are computed. This five step pattern of calculation occurs in other physical problems, and therefore the programming techniques are of general interest.

Referring to Figure 24 the relationship between computer variables in the program segment and physical quantities is depicted in Figure 25. In Figure 24, the second card sets the counting index, PAR, to zero. Card #3 indicates which two Hamiltonian submatrices are going to be calculated - viz. the $J = 2$, $K = 1$, $M_F = 9/2$ submatrix and the $J = 3$, $K = 1$, $M_F = 9/2$ submatrix. Card #4 sets the row index, R1, the column index, C1, and the matrix size index, N, to zero.

Cards #5-8 specify the values of the quantum numbers, F, I, and v that are allowed in a given submatrix. Specifically, F must be in the range $[J + 7/2, |M_F|]$; I must be in the range $[\text{minimum of } (7/2, F+J), |F-J|]$; and v can take on values 0 and 1. Figure 26 shows the submatrix corresponding to $J = 2$, $K = 1$, and $M_F = 9/2$. Card #9 causes the row index to be increased by 1 each time a different combination of the quantum numbers F, I, and v is chosen in a matrix

element calculation.

Cards #10 - 15 specify the allowed values that F' , I' , and v' may have in a given submatrix. However, since the submatrices are symmetric, cards #10-15 only specify matrix elements which are on the diagonal or to the right of it. (See Figure 26.) Card #16 increases the column index by 1 each time a different matrix element is computed in a row. Card #16 also assigns the value C1 to N. Thus, when the last matrix element, $A(N, N)$ is computed the computer variable N specifies the size of the matrix, A.

Cards #17, 18 call a procedure, MATRICELEMENT, to compute the matrix element corresponding to the current values of the quantum numbers M_F , K, J, F, F' , I, I' , v, and v' . The value of this matrix element is assigned to the appropriate element in the matrix, $A(R1, C1)$.

Card #23 calls on the EAGLE procedure. The function of this procedure has already been discussed. Cards #24-43 store the eigenvalues and associated eigenvectors in arrays. For a $J = 2$ submatrix, the eigenvalues are stored in the 1 dimensional array, EGY1 (K1) and the corresponding eigenvectors are stored in the four dimensional array $B1(V1, (I1 + 1)/2, (F1 + 1)/2, K1)$. For a $J = 3$ submatrix, the eigenvector and eigenvector information are stored in EGY2 and B2 arrays. Figure 27 shows the form of the K1-th eigenvector.

Cards #44-62 compute the frequencies and intensities of all transitions between the two submatrices. The energy splittings are given by card #61 $(SPLIT = EGY2[K] - EGY [K1])$ and the intensities are given by card #60 -- which is the computed values of equation III-23 for intensity.

The information computed in cards #60 and 61 is stored in arrays by cards #62-64. Card #62 enumerates the transition whose frequency and intensity has been computed. Card #63 puts the calculated intensity into an intensity array, PEAK. Card #64 puts the calculated splitting into a frequency array, NU. PEAK and NU are two dimensional arrays because the largest size a one dimensional array can have is 1023 elements. Storage of more than this number of frequencies and intensities requires arrays of larger dimensionality.

The DIV, MOD construction used in the Program Segment is not used in PBRTAPE, but it could have been and the result would have been fewer cards. PAR DIV 1000 has the value $\text{PAR}/1000$ rounded down to the nearest lower integer. PAR MOD 1000 has the value $[\text{PAR} - \text{PAR DIV } 1000] \times 1000$. Thus, for example $[2543 \text{ DIV } 1000, 2543 \text{ MOD } 1000] = [2, 543]$.

BEGIN	1.
:	
:	
PAR←0;	2.
MF2←9; KQ←1; FØR JQ←2, 3 DØ BEGIN	3.
R1 ← C1 ← N ← 0;	4.
FØR F1 ← 2 x JQ + 7 STEP -2 UNTIL ABS (MF2) DO BEGIN	5.
MIN 4 ← MIN (7, F1 + 2 x JQ);	6.
FØR I1 ← MIN 4 STEP -2 WHILE I1 ≥ ABS (F1-2xJQ) DØ	7.
FØR V1 ← 0, 1 DØ BEGIN	8.
C1 ← R1; R1 ← R1 + 1;	9.
FØR F2 ← F1 STEP -2 UNTIL ABS (MF2) DØ BEGIN	10.
MIN3 ← MIN (7, F2 + 2 x JQ);	11.
FØR I2 ← IF F2 = F1 THEN I1 ELSE MIN 3 STEP	12.
-2 WHILE I2 ≥ ABS (F2 - 2XJQ) DØ	13.
FØR V2 ← IF F2 = F2 AND I1 = I2 THEN V1 ELSE 0	14.
STEP 1 UNTIL 1 DØ BEGIN	15.
C1 ← C1 + 1; N ← C1;	16.
A [R1, C1] ← MATRIXELEMENT(MF2/2, KQ, J,	17.
F1/2, F2/2, I1/2, I2/2, V1, V2);	18.
END;	19.
END;	20.
END;	21.
END;	22.
EAGLE (N, A);	23.
FØR K1 ← 1 STEP 1 UNTIL N DØ BEGIN	24.
I ← 0;	25.
FØR F1 ← 2 x JQ+7 STEP -2 UNTIL ABS(MF2) DØ BEGIN	26.
MIN 4 ← MIN (7, F1 + 2 x JQ);	27.
FØR I1 ← MIN4 STEP -2 WHILE I1 ≥ ABS (F1 - 2xJQ) DØ	28.

Figure 24. Program Segment (Continued).

```

FØR V1 ← 0, 1 DØ BEGIN                                29.
    I ← I + 1                                           30.
    IF JQ = 2 THEN BEGIN                                31.
        B1 [ V1, ( I + 1 ) / 2, (F1+1)/2, K1] ← DG[ I, K 1] ; 32.
        EGY1 [ K1] ← A [ K1, K1] ;                     33.
        N1 ← N;                                         34.
    END;                                                 35.
    IF JQ = 3 THEN BEGIN                                36.
        B2 [ V1, (I + 1)/2, ( I + 1)/2, K1] ← DG[ I, K1] ; 37.
        EGY2 [ K1] ← A [ K1, K1] ;                     38.
        N2 ← N                                          39.
    END;                                                 40.
END;                                                     41.
END;                                                     42.
END;                                                     43.
FØR K1 ← 1 STEP 1 UNTIL N1 DØ                            44.
FØR K2 ← 1 STEP 1 UNTIL N2 DØ BEGIN                      45.
    SUM I ← 0;                                          46.
    FØR F2 ← (2 x 3 + 7) STEP - 2 UNTIL ABS (MF2) DØ    47.
    FØR F1 ← (2 x 2+7) STEP -2 UNTIL ABS (MF2) DØ BEGIN 48.
        MIN 4 ← MIN 2 (7, F1 + 2 x 2, F2 + 2 x 3, 20); 49.
        FØR I1 ← MIN 4 STEP - 2 WHILE I1 ≥ ABS (F1 - 2 x 2) 50.
        AND I1 ≥ ABS (F2 - 2 x 3) DØ                    51.
        FØR V1 ← 0, 1 DØ BEGIN                          52.
            V2 ← IF V1 = 0 THEN 1 ELSE 0;                53.
            TB1 ← B1 [ V1, (I + 1)/2, (F1 + 1)/2, K1] ; 54.
            TB2 ← B2 [ V2, (I1 + 1)/2, (F2 + 1)/2, K2] ; 55.
            SUM I ← SUM I + TB1 x TB2 x D [ V1, V2, KQ, 56.
            MF2/2, F1/2, F2/2, I 1] ;                   57.
        END;
    END;
END;

```

Figure 24. Program Segment (Continued).

END;	58.
END;	59.
INT ← SUM I* 2 ;	60.
SPLIT ← EGY 2 [K2] - EGY 1[K1] ;	61.
PAR ← PAR + 1 ;	62.
PEAK [PAR DIV 1000, PAR MOD 1000] ← INT;	63.
NU [PAR DIV 1000, PAR MOD 1000] ← SPLIT;	64.
IF I NT ≥ 0.01 THEN WRITE (LINE, SOMETHING, SPLIT, INT, PAR);	65.
END;	66.
END;	67.
⋮	
END.	68.

Figure 24. Program Segment (Concluded).

-
1. PAR = an index used to enumerate each transition.
 2. MF2 = $2 \times M_F$, where M_F is the azimuthal quantum number.
 3. KQ = K, where K is the quantum number specifying the projection of angular momentum along the molecular z axis.
 4. JQ = J, the rotational quantum number.
 5. R1, C1 = the row and column indice of the array A [R1, C1] .
 6. N = the size of the NxN matrix A [R1, C1] .
 7. F1 = twice the quantum number F.
 8. I 1 = twice the quantum number I.
 9. V1 = the quantum number V.
 10. F2 = twice the quantum number F.
 11. I 2 = twice the quantum number I.
 12. V2 = the quantum number V.
 13. I = an integer used to locate the eigenvector column in DG [I, K1] corresponding to the eigenvalue A[I, I] .
 14. K1 = counting index for J = 2 eigenvalue.
 15. K2 = counting index for J = 3 eigenvalue.
 16. N1 = total number of J = 2 eigenvalues.
 17. N2 = total number of J = 3 eigenvalues.

Figure 25. Computer Variables and Associated
Physical Quantities

18. TB1, TB2 = temporary storage for B1 ... and B2 ... , results in
faster evaluation of arithmetic expression in cards #56,57.
19. SUM I = temporary storage for a real variable.
20. INT = intensity of a transition being considered.
21. SPLIT = frequency of a transition being considered.
-

Figure 25. Computer Variables and Associated
Physical Quantities (Concluded)

			F	=	11/2	11/2	9/2	9/2	9/2	9/2	9/2
			I	=	7/2	7/2	7/2	7/2	5/2	5/2	5/2
			V	=	0	1	0	1	0	1	1
F	I	V									
11/2	7/2	0	A[1, 1]	A[1, 2]	A[1, 3]	A[1, 4]	A[1, 5]	A[1, 6]			
11/2	7/2	1	.	A[2, 2]	A[2, 3]	A[2, 4]	A[2, 5]	A[2, 6]			
9/2	7/2	0	.	.	A[3, 3]	A[3, 4]	A[3, 5]	A[3, 6]			
9/2	7/2	1	.	.	.	A[4, 4]	A[4, 5]	A[4, 6]			
9/2	5/2	0	A[5, 5]	A[5, 6]			
9/2	5/2	1	A[6, 6]			

Figure 26. The $J = 2$, $M_F = 9/2$, $K = 1$ Submatrix.

EIGENVECTOR (corresponding to K_1 -th eigenvalue) =

$$\begin{aligned}
 & B_1[0, 4, 6, K_1] u(11/2, 7/2, 0) + B_1[1, 4, 6, K_1] u(11/2, 7/2, 1) \\
 & + B_1[0, 4, 5, K_1] u(9/2, 7/2, 0) + B_1[1, 4, 5, K_1] u(9/2, 7/2, 1) \\
 & + B_1[0, 4, 5, K_1] u(9/2, 5/2, 0) + B_1[1, 3, 5, K_1] u(9/2, 5/2, 1)
 \end{aligned}$$

where $u = u(F, I, v)$.

Figure 27. Form of Eigenvector Corresponding to K_1 -th Eigenvalue

of the $J = 2$, $K = 1$, $M_F = 9/2$ Submatrix.

LITERATURE CITED

1. A. A. Wolf, Ph.D. Thesis, Georgia Institute of Technology (1966).
2. C. R. Nave, Ph.D. Thesis, Georgia Institute of Technology (1966).
3. K. K. Svidzinski, "Theory of the Hyperfine Structure in the Rotational Spectra of Molecules," Soviet Maser Research, ed. D. V. Skobel'tsyn (Consultants Bureau, New York, 1964).
4. A. L. McClellan, Tables of Experimental Dipole Moments (W. H. Freeman and Company, San Francisco and London, 1963), p. 37.
5. C. H. Townes and A. L. Schawlow, Microwave Spectroscopy (McGraw-Hill Book Co., Inc., New York, 1955), p. 268.
6. J. H. N. Loubser, J. Chem. Phys. 36, 2808 (1962).
7. M. Jen and D. R. Lide, Jr., J. Chem. Phys. 36, 2525 (1962).
8. P. N. Wolfe, J. Chem. Phys. 25, 976 (1956).
9. M. W. Long, J. Chem. Phys. 33, 508 (1960).
10. A. A. Wolf, J. Chem. Phys. 47, 5101 (1967).
11. L. Clayton, Ph.D. Thesis, Georgia Institute of Technology (1961).
12. M. W. Long, Ph.D. Thesis, Georgia Institute of Technology (1959).
13. C. R. Nave, op cit., p. 49.
14. A. Narath and W. D. Gwinn, The Review of Scientific Instruments 33, 79 (1962).
15. C. R. Nave, op. cit., p 13ff.
16. A. R. Edmonds, Angular Momentum in Quantum Mechanics, (Princeton University Press, Princeton 1960), p. 72 and 115.
17. A. A. Wolf, J. Chem. Phys. 47, 5102 (1967).

18. Svidzinski, op. cit., p. 112.
19. A. A. Wolf, op. cit., p. 5103.
20. Manuel Rotenberg, R. Bivens, N. Metropolis, John K. Wooten Jr., The 3-j and 6-j symbols (The Technology Press. Massachusetts Institute of Technology, Cambridge, Mass. 1959).
21. M. Hammermesh, Group Theory and Its Applications to Physical Problems (Addison-Wesley Publishing Co., Inc., Reading, Mass., 1962), p. 161.
22. A. A. Wolf, op. cit., p. 5104.
23. A. A. Wolf, op. cit., p. 5104.
24. A. A. Wolf, Ph.D. Thesis, Georgia Institute of Technology (1966), p. 54.
25. A. A. Wolf, op. cit., p. 58.
26. C. R. Nave, op. cit., p. 44.
27. C. R. Nave, op. cit., p. 48.
28. C. H. Townes and A. L. Schawlow, op. cit., p. 96.
29. C. R. Nave, op. cit., p. 55.
30. C. R. Nave, op. cit., p. 54.
31. A. A. Wolf, Ph.D. Thesis, Georgia Institute of Technology (1966), p. 81.
32. A. A. Wolf, op. cit., p. 75.
33. C. H. Townes and A. L. Schawlow, op. cit., pp. 338-348.

VITA

Philip Benton Reinhart was born on March 17, 1939 in Philadelphia, Pennsylvania. He graduated from the Taft School in Watertown, Connecticut in 1957. He received the Bachelor of Science degree in 1961 and the Master of Science degree in 1963 from Yale University in physics.

He has been a physics instructor at Agnes Scott College since the fall of 1963. At Georgia Institute of Technology as a full or part time student since 1964, he received a National Science Foundation Science Faculty Fellowship for graduate study from June 1967 to June 1968 and has been on leave from Agnes Scott College for that period.

In September, 1968 Mr. Reinhart returns to Agnes Scott College as an Assistant Professor in Physics.